arXiv:2211.12410v2 [astro-ph.EP] 3 Oct 2023

Pre-solar grains from novae and "Born-again giants"

A. Evans[a], R. D. Gehrz[b]

[a]*Astrophysics Group, Lennard-Jones Laboratories, Keele University, Keele, Staffordshire, ST5 5BG, UK*
[b]*Minnesota Institute for Astrophysics John T. Tate Hall 116 Church St. SE Minneapolis, MN 55455, USA*

Abstract

We review the properties of dust formed during classical nova eruptions and the Very Late Thermal Pulses (VLTPs) that occur during the later stages of post-Asymptotic Giant Branch evolution of low-mass stars. In both cases, carbon and hydrocarbon dust is produced. Novae may also produce silicate dust, contrary to the usual paradigm about the C:O ratio and dust composition. Despite the expectation that these dust sources are not expected to make significant contributions to the Galactic dust population, there is a significant body of evidence that grains from both stellar sources have been identified in recovered meteoritic and cometary material, and that certain infrared spectral signatures seen in comets are common to novae, VLTPs and pre-solar grains.

Keywords: Novae — Very Late Thermal Pulses — Circumstellar dust — cometary dust — pre-solar grains

Contents

1 Introduction **2**

2 Nova eruptions **3**
2.1 The eruption 3
2.2 Abundances in the ejecta 4
2.3 The route to dust formation 5
2.4 The nature of the dust in novae 14
2.4.1 Silicate dust 14
2.4.2 Hydrocarbons 19

2.5 Summary 20

3 "Born-again" giants 22
3.1 The Very Late Thermal Pulse 22
3.2 Summary 25

4 The pre-solar connection 25
4.1 Novae 26
4.2 Born-Again Giants 31

5 Some speculative (and provocative) concluding remarks 34

1. Introduction

Nova eruptions and Very Late Thermal Pulses (VLTPs) in low mass stars originate on the surfaces of degenerate objects: white dwarfs (WDs) in binary systems in novae, and on top of the degenerate cores of Asymptotic Giant Branch (AGB) stars in VLTPs. In novae and VLTPs the nuclear burning leads to an eruption, which is explosive in the case of novae. When VLTPs are reported, it is common for them to be described as a "nova". For example the VLTP V4334 Sgr[1] (known as Sakurai's Object, in honour of its discoverer, the amateur astronomer Yukio Sakurai) was, until 2021, still listed in the SIMBAD[2] database as a "nova-like star"; at the time of this writing it is listed as a "Cataclysmic Variable Star", which is somewhat less inaccurate.

Evidence in Solar System material for "stardust", grains produced in stellar winds, comes from (a) laboratory studies of recovered material (such as meteorites and interplanetary dust particles, hereafter IDPs), in which elemental and isotopic signatures are identified and (b) spectroscopic observations, comparing (especially) infrared (IR) spectra of Solar System objects and extra-solar proto-planetary systems with the IR spectra of the sources of stardust. Regarding elemental and isotopic abundances, it is preferable to have agreement between predicted and measured values for as many species as possible in order to discriminate between stellar sources. For example, the $^{12}C/^{13}C$ ratio for both novae and VLTPs is predicted to be $\lesssim 10$ (see below).

[1] In general, variable star names in this chapter follow the convention recommended by the International Astronomical Union.

[2] http://simbad.u-strasbg.fr/simbad/

In this chapter we briefly describe the causes of nova and VLTP eruptions, the way in which the eruption progresses, the nature of the ejected material and of the dust formed. In each case we describe the evidence indicating that these systems contributed to the material from which the Sun and its entourage formed.

Given the considerable history of observation and theory for novae by comparison with VLTPs, our discussion is heavily biased towards novae.

2. Nova eruptions

2.1. The eruption

Classical nova eruptions occur in semi-detached binary systems consisting of a WD primary and a late-type secondary (see comprehensive reviews by Bode & Evans, 2008; Saikia & Anupama, 2012; Woudt & Riberio, 2014). The WD may be of "CO" or of "ONe" type, the latter generally, but not exclusively, being at the high-mass end of WD masses. The late-type star is usually a main sequence dwarf, but nova systems are known that have sub-giant secondaries (e.g., GK Per; Kraft, 1964).

The secondary star fills its Roche lobe; material from the secondary flows onto the surface of the WD through the inner Lagrangian point, and spirals onto the WD surface as an accretion disk. In time the material at the base of the accreted layer becomes degenerate, and hot enough to initiate hydrogen burning. A Thermonuclear Runaway (TNR) ensues, resulting in the explosive ejection of some 10^{-6}–$10^{-4}\,M_\odot$ of material, at several 100 to several $1000\,km\,s^{-1}$. As a result of the TNR, and the ingestion of some WD material into the TNR region, the ejected material is enriched in C, N, O, Mg, Si, Al, Ne, and other metals. See Jordi José's contribution to this volume (Chapter 9), and references therein, for a full discussion of the TNR.

The ejecta, both as gas and dust that condenses as the expanding ejecta cool, enrich the interstellar medium. Moreover, the TNR imprints nova-specific isotopic ratios on the ejecta, and it is likely that classical nova explosions are a major source of Galactic ^{13}C, ^{15}N and ^{17}O (see Gehrz et al., 1998). It has also been suggested that novae might make a significant contribution to Galactic ^{7}Li (Starrfield et al., 2020, and references therein), although the case is far from clear (José et al., 2020, and Chapter 9).

In time (typically $\sim 5-10$ years), the eruption subsides and mass-transfer resumes. The accretion disk is re-established until the conditions again arise for another TNR to occur, after an interval of $\sim 10^4 - 10^5$ years. All novae

are therefore recurrent, but where the secondary is a red giant the recurrence time-scale is less than a human lifetime, so these systems are seen by humans to erupt more than once; these are the "recurrent novae" (RNe; see Evans et al., 2008). In general, these are not dust-formers, although there was an extremely transient phase of CO and dust formation during the 2014 eruption of the RN V745 Sco (Banerjee et al., 2023). The recurrent nova RS Oph displays strong 9.7 μm and 18 μm silicate features, which are associated with the red giant secondary (Evans et al., 2007). Henceforth we largely confine our discussion to classical novae.

The mass-loss from a nova eruption is in the form of a continuous but diminishing wind that originates on the WD surface (Bath & Shaviv, 1976). A key property of classical nova eruptions is that, to a good approximation, the *bolometric* luminosity $L_{\rm bol}$ of the stellar remnant remains $\sim$ constant throughout the eruption (as was first shown theoretically by Bath & Shaviv, 1976); this constant bolometric luminosity is of the order of, or may exceed, the Eddington luminosity for the WD. Thus as the pseudo-photosphere of the ejecta shrinks back onto the surface of the WD as the mass-loss rate diminishes, the effective temperature increases to maintain constant $L_{\rm bol}$. The well-known visual light decline of an erupting nova is therefore simply a bolometric correction effect as the maximum of the spectral energy distribution (SED), which is roughly Planckian, shifts out of the visible, into the ultra-violet and eventually X-rays. The visual magnitude falls as the Rayleigh-Jeans tail slides through the visible window toward short wavelengths (Bath & Shaviv, 1976; Gallagher & Starrfield, 1976).

2.2. Abundances in the ejecta

The composition of the ejecta from a nova eruption is determined, amongst other factors, by the composition of the secondary star (material from the surface of which is deposited on the surface of the WD), the nature of the WD itself (i.e. whether it is of CO or ONe type), and how much mixing of the WD and accreted material occurs. Moreover, the composition (both elemental and isotopic) of the ejecta are important in that they may have infiltrated material that produced the proto-solar nebula: analysis of material from meteorites and IDPs may reveal the extent to which this may have occurred.

Simulations for CO and ONe WDs (Starrfield et al., 2009, 2020), giving the yield in mass fraction, expressed relative to solar abundances, are shown in Fig. 1. We note here that care should be taken in directly comparing

published yields expressed in this way, to ensure that the solar benchmarks are the same; for example, in Fig. 1, the solar reference values are from Anders & Grevesse (1989) (ONe) and Lodders (2003) (CO) respectively.

We see from Fig. 1 that large overabundaces of CNO are predicted for CO WDs, suggesting that carbon is a plausible dust composition for these novae[3]. Likewise, large overabundaces of Ne, Na, Si, Al, P and S are predicted for ONe WDs. A large overabundance of Ne was first deduced for nova V1500 Cyg (Ferland & Shields, 1978a,b), giving rise to the concept of "neon novae" originating from a TNR on an ONe WD. The implication is that there is mixing of the WD and accreted material. The discovery of large overabundances of Ne in nova ejecta are now relatively commonplace (e.g., QU Vul, Gehrz et al., 2008, and references therein).

Once the ejected material is ionised and excited by the hot stellar remnant, the nova enters a "nebular" phase, in which the spectrum at all wavelengths is dominated by strong ionic emission lines (see e.g., Fig. 6 below). At this time, analysis of the line fluxes using photoionisation codes such as CLOUDY (Ferland et al., 2017) allows the determination of elemental abundance relative to hydrogen. The observations, followed by detailed analysis, largely confirm the predictions from TNR theory.

Several authors (e.g., José et al., 2004; Starrfield et al., 2009, 2020, and references therein) have also calculated detailed isotopic ratios for a variety of TNRs, on CO and ONe WDs having a range of masses. A summary of typical values is shown in Fig. 2 (from José et al., 2004). These authors find that, for ONe novae, significant overabundances of ^{15}N and ^{17}O are produced, while CO novae may produce significant amounts of ^{7}Li (but see comment in Section 2.1). In the latter novae ^{12}C/^{13}C is < 1 for CO WD masses in excess of $0.8\,M_{\odot}$. As pointed out by Gehrz et al. (2008), a significant amount of ^{22}Ne could arise from the radioactive decay of ^{22}Na (β^{+} active, half-life 2.60 years) produced in the TNR, which is also predicted to be overabundant in neon novae.

2.3. The route to dust formation

Nova eruptions that occur in systems having CO WDs frequently produce dust in their ejecta. The evidence for dust formation originally came

[3]Note that these simulations also show an overabundance of C in ONe novae (see Fig. 1), but ONe novae are generally less proficient dust producers (Gehrz et al., 1998; Evans & Gehrz, 2012).

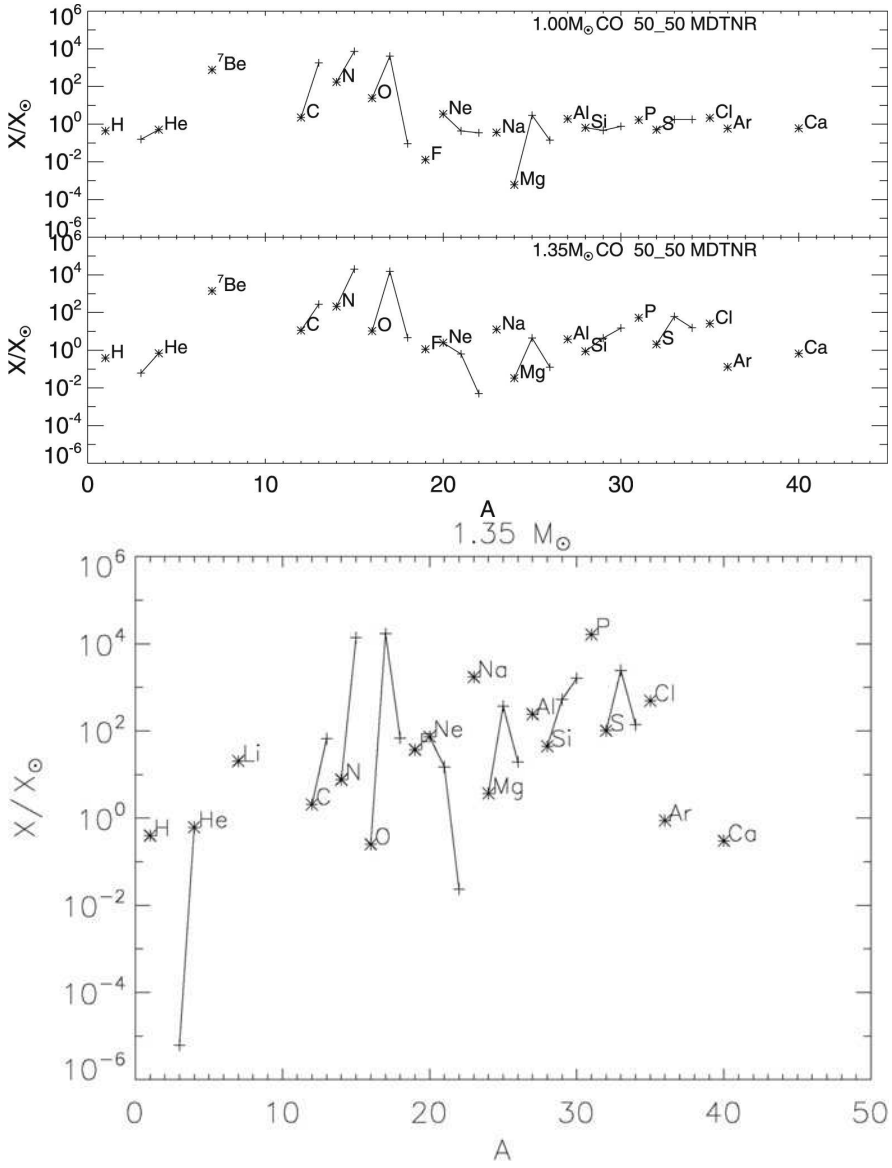


Figure 1: Ejecta abundances (by mass) for stable isotopes, from H to Ca, for a TNR on the surface of a WD in a nova system. A is the atomic mass; the y-axis is the logarithmic ratio of the ejecta abundances divided by the corresponding solar abundances. Top panel: $1.0\,M_\odot$ (top) and $1.35\,M_\odot$ (bottom) CO WD, with a 50:50 mix of WD and accreted material. Solar abundances from Lodders (2003). Bottom panel: $1.35\,M_\odot$ ONe WD, with a 50:50 mix of WD and accreted material; solar abundances from Anders & Grevesse (1989). The most abundant isotope of a given element is designated by an asterisk; all isotopes of a given element are connected by solid lines. Figures from Starrfield et al. (2020) (top) and Starrfield et al. (2009) (bottom). ©AAS. Reproduced with permission.

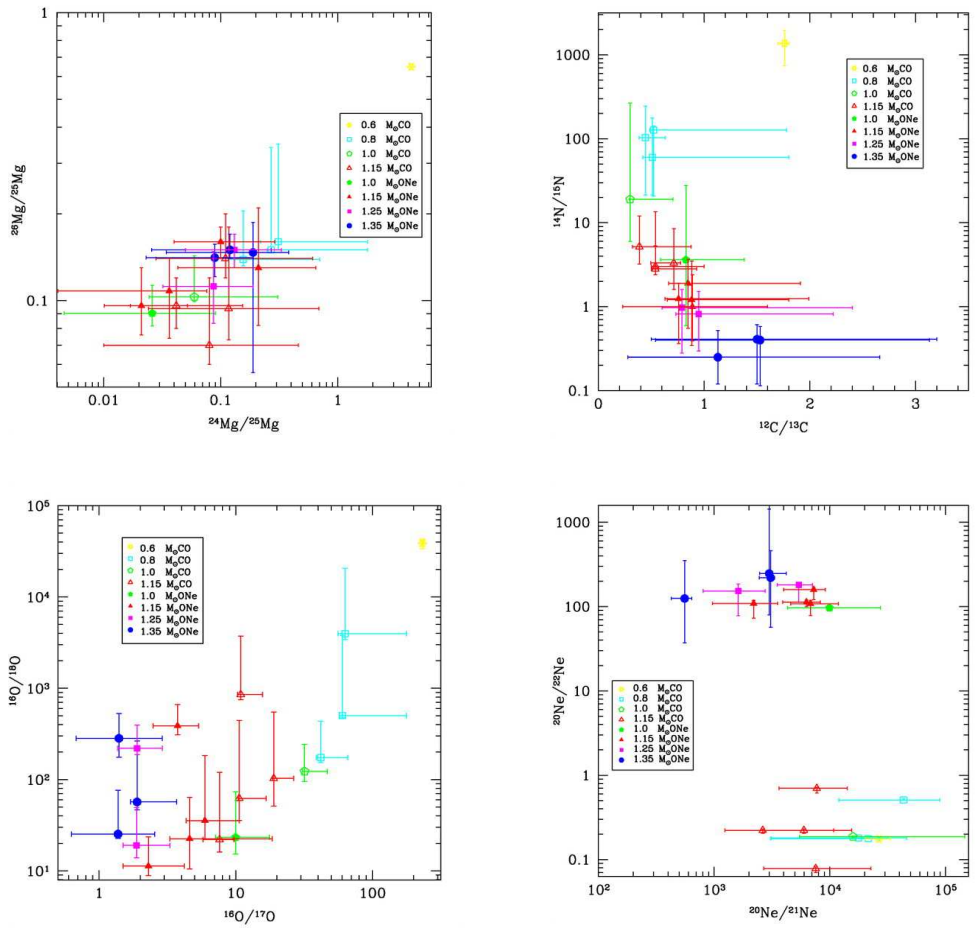


Figure 2: Predicted isotopic ratios for TNR for a variety of WD types (CO/ONe) and masses. "Error bars" take into account the composition gradient in the ejected shells. From José et al. (2004). ©AAS. Reproduced with permission.

from the deep minimum in the visual light curve, first noted in nova DQ Her 1934 (see Strope et al., 2010) in which the dust minimum was $\sim$ 10 mag deep. Around the time of the DQ Her eruption, the deep minima in the light curves of R Coronae Borealis stars (see e.g., Clayton, 2012) was being attributed to obscuration by dust (Loreta, 1935; O'Keefe, 1939). By analogy with the R CrB stars, it was McLaughlin (1935) who first suggested that the deep minimum in the visual light curve of DQ Her was due to the formation of dust in the ejected material. However it was not until the seminal observations by Geisel et al. (1970) that confirmation of this hypothesis came with the detection of a large IR excess in the dust-forming nova FH Ser 1970, that coincided with a deep minimum in its visual light curve. Advances in our understanding of the IR temporal development of novae have been reviewed by Gehrz et al. (1998), Gehrz (2008), Banerjee & Ashok (2012) and Evans & Gehrz (2012).

There is (as yet) no unbiassed sample of nova light curves[4], but the sample in Strope et al. (2010) probably comes closest at the time of this writing. The sample compiled by Strope et al. suggests that the light curves of about 20% of classical novae show evidence of deep dust minima, although as many as 30% of classical novae are dust-producers. In some cases, the apparent discrepancy likely arises becaue the dust distribution is highly anisotropic (as in the case of V1280 Sco; Chesneau et al., 2012): if the optically thick part of the dust shell happens not to lie along the line-of-sight then only a mild dip in the visual light curve occurs, even though there may be a substantial IR excess. In other cases, such as V1668 Cyg (Gehrz et al., 1980b), a smaller amount of dust forms than in the case of novae like V705 Cas (see Fig. 3, adapted from Mason et al., 1998) that show deep visual minima during dust formation.

When the ejecta reach a nominal condensation distance for a specific condensate, then dust condensation may occur if the gas density in the ejected shell is high enough. A necessary condition is the formation of nucleation sites and, before that, the formation of small molecules such as CO and C_2. First overtone CO emission has frequently been detected in erupting novae (see Banerjee et al., 2016, and references therein). That paper (their Table 9) also summarises the values of the $^{12}C/^{13}C$ ratio in novae, as determined from

[4]This situation is of course very likely to change when the Legacy Survey of Space and Time (LSST) of the Vera C. Rubin Observatory (Lund et al., 2016) becomes operational.

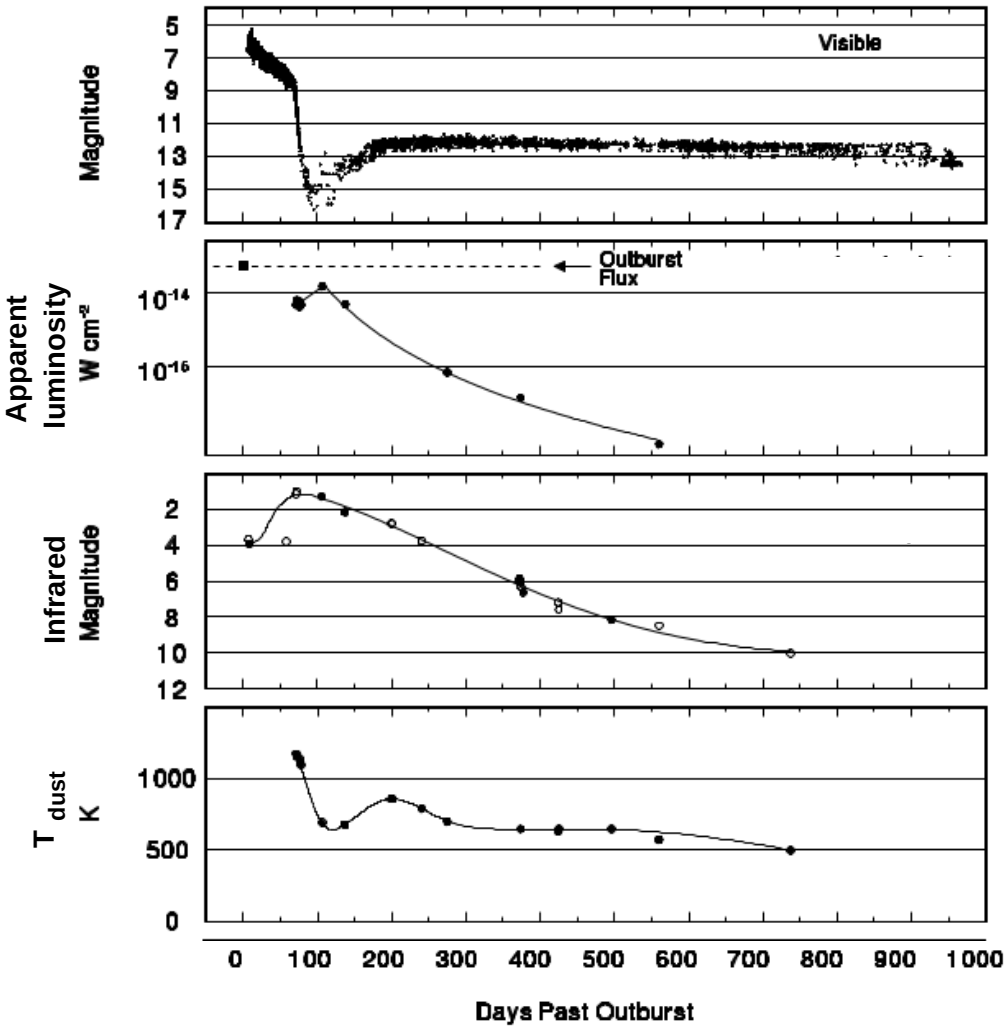


Figure 3: Temporal development of nova V705 Cas. Top and next-to-bottom panels illustrate respectively the drop in the visual and the concurrent rise in the IR as dust formation occurs. IR magnitudes at 3.6 μm are shown as filled circles; open circles are IR magnitudes at 3.8 μm. The dust temperature is given in the bottom panel. Figure adapted from Mason et al. (1998). ©AAS. Reproduced with permission.

the CO isotopologue emission. This shows that the ratio is close to unity, and far less than the Solar System value of $\sim$ 89 (Asplund et al., 2009). Furthermore, it is evident that, for $^{12}C/^{13}C$ at least, the observations confirm the predictions of the TNR models.

Other diatomic molecules detected in novae include CN and C_2 (Nagashima et al., 2014; Kawakita et al., 2015; Fujii et al., 2021, see also references in Evans & Rawlings (2008)). Other than $^{12}C/^{13}C$, there have been few determinations of isotopic ratios in nova ejecta; while Pavlenko et al. (2020) present isotopic ratios for C, O and Si for the RN T CrB, the situation is complicated by the fact that the ratios are for the photosphere of the red giant secondary, onto which the products of the TNR on the nearby WD have been entrained.

The environment of a nova, with its intense ultra-violet radiation field, shocks etc., is extremely hostile to small molecules and nucleation sites, and it is very likely that molecule and grain formation occur in dense clumps, similar to those seen in the Helix Nebula (NGC 7293; Hora et al., 2006). Indeed clumps with extended tails, similar to those in the Helix, are seen in the ejected shell of DQ Her (Vaytet et al., 2007).

Detailed analysis of the formation of small molecules in nova ejecta has been carried out by Rawlings (1988), Rawlings & Williams (1989), and Pontefract & Rawlings (2004). Rawlings & Williams have followed the chemical networks as far as the formation of small carbon clusters, C_n, with n as large as 8. Derdzinski et al. (2017) have shown that radiative shocks in nova ejecta can result in the high densities required for the formation of CO and of the requisite nucleation sites.

The usual paradigm is that O-rich condensates (e.g. silicates) form in an environment in which C<O by number, while C-rich condensates (e.g. carbon, SiC) form when C>O. Many TNR models predict that nova ejecta are O-rich. However, José et al. (2016) explored the effect of the WD composition on the outcome of the TNR, for a WD progenitor having mass $8\,M_\odot$. These profiles lead to C-rich (rather than O-rich) ejecta. Whether the ejecta are O- or C-rich seems to depend critically on the composition of the outer WD shell. Notwithstanding these issues, the above dust condensation paradigm does not apply in novae as it is common to find that dust-forming novae form both types of condensate in the course of the same eruption (see e.g. Evans & Rawlings, 2008, and references therein). Examples of this behaviour include V705 Cas (Evans et al., 1997, 2005; Gehrz et al., 1995), V842 Cen (Hyland & McGregor, 1989; Smith et al., 1994), QV Vul, V1065 Cen (Helton et al., 2010), and V5668 Sgr (Gehrz et al., 2018). Of the

these, V842 Cen, QV Vul, and V705 Cas had deep minima in their visual light curves whereas V1065 Cen had a more modest dip.

The significance of the C:O ratio is that, whichever of C and O has the lower abundance is locked up in the CO molecule, which is very stable at the temperatures ($\lesssim$2000 K) at which grains form. This may indicate that CO formation does not go to saturation, so that both C and O are available for incorporation into dust, or that there are steep abundance gradients in the ejecta, such that the C:O ratio varies as a function of location.

Table 1: Indicative values of dust masses in nova ejecta. A bullet (•) indicates that the component was present but there is no mass estimate.

Nova	Year of outburst	Dust mass ($10^{-8}\,M_\odot$) Carbon	Silicate	Total	Aromatic IR features	Reference
NQ Vul	1976	35				Ney & Hatfield (1978)
LW Ser	1978	160				Gehrz et al. (1980a)
V1668 Cyg	1978			2.5		Gehrz et al. (1980b)
V1370 Aql	1982		•	40–2000		Snijders et al. (1987)
						Bode et al. (1984)
QU Vul	1984		1			Gehrz et al. (1986)
QV Vul	1984			100	•	Gehrz et al. (1992)
V842 Cen	1986	5	20		•	Hyland & McGregor (1989)
						Smith et al. (1994)
V838 Her	1991		0.48		•	Woodward et al. (1992)
V705 Cas	1993	60–82	7		•	Gehrz et al. (1995)
						Mason et al. (1998)
V1424 Aql	1995			17–80		Mason et al. (1996)
V5668 Sgr	2005			12		Gehrz et al. (2018)
V2361 Cyg	2005				•	Helton et al. (2011)
V2362 Cyg	2006				•	Helton et al. (2011)
V1065 Cen	2007		•	2–37		Helton et al. (2010)
V1280 Sco	2007	6.6–8.7	34–43		•	Sakon et al. (2016)
V339 Del	2015	12				Gehrz et al. (2015)
		2.7				Evans et al. (2017)
V5668 Sgr	2015	12	•			Gehrz et al. (2018)

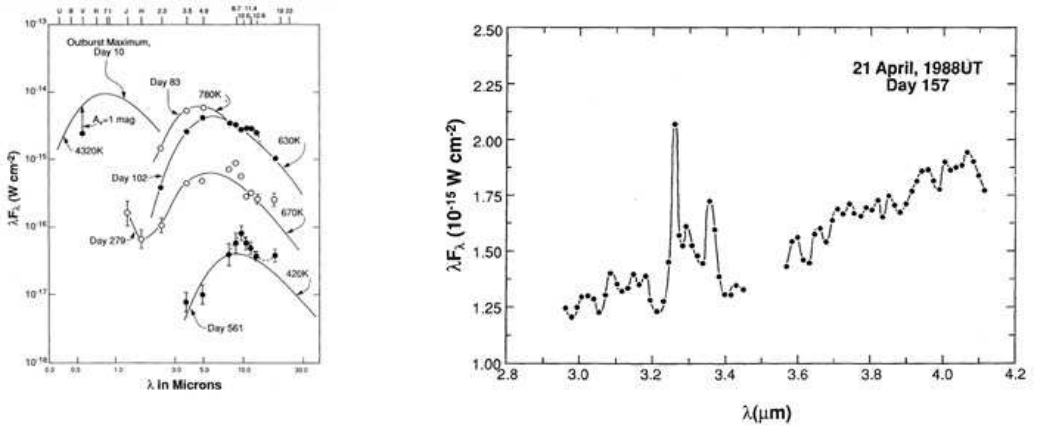


Figure 4: Evidence for the formation of four different mineral compositions in nova QV Vul. Left panel: Spectral energy distributions indicating the presence of carbon, SiC and silicates at various phases of the temporal development of the nova. Right panel: The 3.2 μm emission feature indicates the presence of hydrocarbons. Figures from Gehrz et al. (1992). ©AAS. Reproduced with permission.

An extreme example of this behaviour was seen in QV Vul (see Fig. 4; Gehrz et al., 1992). On the evidence of the visual light curve, dust formed in the ejecta of this nova at $\sim$ 50 days after the eruption. Carbon dust was first identified at 83 days, and was present throughout the 2 years of observation. SiC (11.3 μm) appeared at 102 days, and the 9.7 and 19.5 μm silicate features on day 561.

The mass of dust produced may be estimated if (a) the emissivity of the dust and (b) the distance to the nova are known. Both of these quantities can be subject to large uncertainties, although the situation with regard to distances has improved considerably with data from the *Gaia* mission (Schaefer, 2018; Gaia Collaboration, 2020). Nevertheless the dust masses are plausibly consistent with the deduced masses of ejected gas and a reasonable gas-to-dust ratio. A selection of dust masses determined for the ejecta of several novae is given in Table 1. It should be borne in mind that these masses were determined in various ways, from various data-sets, and some give total dust mass, whatever the dust composition. Also, detailed information about dust mineralogy became available only after the availability of data at reasonably high spectral resolution; earlier studies therefore provide little or no information about the nature of the dust. The data in Table 1 are given here only to give an indication of the range of dust masses and compositions, and are

not meant to be a rigoroursly defined sample.

However, these data enable us to estimate the rate at which nova dust is dispersed into the interstellar medium. Determining the Galactic nova rate is not straight-forward, and recent studies (Shafter, 2017; De et al., 2021) suggest ~ 50 yr^{-1}. If 30% of these produce $\sim 10^{-6}\,M_\odot$ of dust (cf. Table 1) then $\sim 1.5\times10^{-5}\,M_\odot$ of nova dust, of all types, is ejected into the interstellar medium per year.

2.4. The nature of the dust in novae

The early IR observations of novae during their dust phase were broad-band photometry, which gives very little information about the nature of the dust, other than that the spectral energy distribution resembled a featureless black body with a temperature that declines as the dust moves away from the site of the explosion (see Fig. 3). In view of the expected overabundance of carbon in nova ejecta (see Section 2.2). the natural conclusion was that the dust consisted primarily of amorphous carbon. The formation of carbon dust in nova ejecta was first explored in detail by Clayton & Wickramasinghe (1976).

With the advent of IR spectroscopy at moderate resolution, more detailed information was available about the mineralogy of the dust. In particular the InfraRed Spectrograph (IRS; Houck et al., 2004) on the *Spitzer Space Telescope* (Werner et al., 2004; Gehrz et al., 2007) has provided a rich source of information about the mineralogy of nova dust.

2.4.1. Silicate dust

The usual signature of silicate dust is emission in the 9.7 μm Si–O stretch and 18 μm O–Si–O bend modes. However these features are not good diagnostics for the precise mineralogy of the silicate as the 9.7 and 18 μm features are, by their nature, common to all silicates. Discrimination between the various flavours of silicate (e.g. enstatite forsterite, diopside) generally requires high signal-to-noise spectroscopy beyond $\sim 30\,\mu$m (Molster et al., 2002), data that are not yet available for novae.

Nevertheless there do indeed occur variations in the 9.7 μm silicate feature in novae, as seen in Fig. 5 (from Evans et al., 1997, and references therein), which shows the 9.7 μm feature in three novae: V838 Her, V705 Cas and V1370 Aql. It is clear that the features in V838 Her and V1370 Aql were broadly similar, and much broader than that in V705 Cas. Smith et al. (1994) attributed the breadth of, and structure in, the 9.7 μm feature in

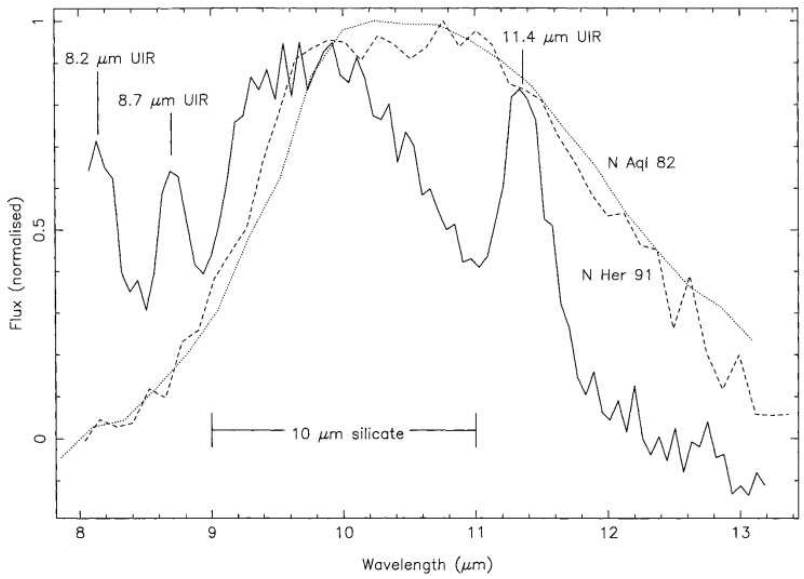


Figure 5: The 9.7 μm silicate features in V838 Her (broken line), V1370 Aql (dotted line) and V705 Cas (solid line), from Evans et al. (1997). Note the "UIR" hydrocarbon features (referred to as AIR in this chapter) superimposed on the silicate feature in V705 Cas. Reproduced with the permission of A. Evans.

novae to a degree of crystallinity, whereas the narrowness of the feature in V705 Cas suggests that the silicate in this nova was amorphous. The latter also showed a very weak 18 μm feature, which Evans et al. (1997) attributed to the fact that the dust was freshly-formed. This conclusion was based on the laboratory work of Nuth & Hecht (1990), who found that the strength of the 18 μm feature relative to that of the 9.7 μm feature strengthens as the dust is annealed.

Fig. 6 shows the *Spitzer* IRS spectrum of nova V1065 Cen, which displays strong evidence for silicate dust, superposed on a continuum that appears to arise from amorphous carbon. However, analyis by Helton et al. (2010) of the dust emission using the DUSTY code (Ivezić et al., 1999) suggested that the dust was dominated by silicate, with little if any contribution from amorphous carbon. In particular there were no hydrocarbon emission features (see below) in this nova. The prominence of neon lines in this nova indicate that it was a neon nova that originated on an ONe WD[5].

[5]The prominence of neon lines is a necessary, but not sufficient, condition, that a nova be classified as a "neon nova", which requires a neon overabundance relative to solar of $\gtrsim 10$ (Helton et al., 2012).

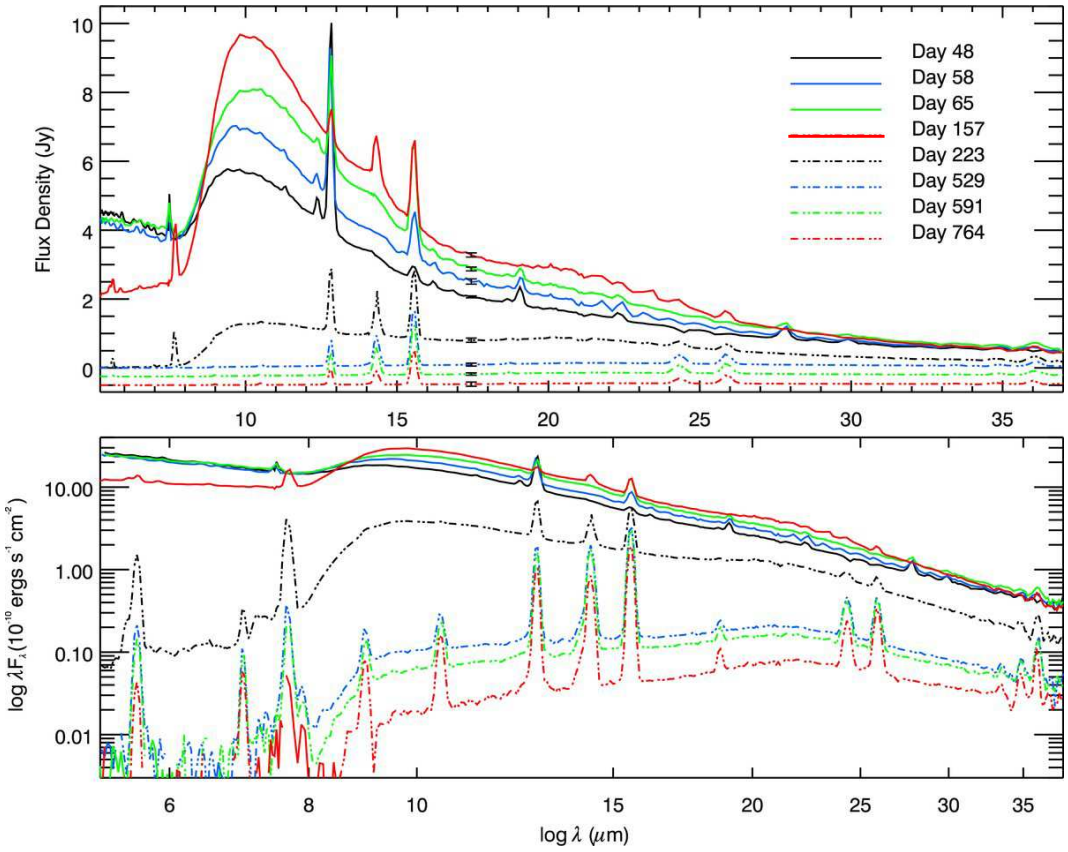


Figure 6: The evolving spectral energy distribution of the newly formed dust around nova V1065 Cen. Note the strong ionic emission features superimposed on the dust continuum, at 7.6 μm ([Ne VI]), 12.8 μm ([Ne II]), 13.5 μm ([Mg V]), 15.5 μm ([Ne III]), 14.3 μm, 24.3 μm ([Ne V]) and 25.9 μm ([O IV]). There are also hydrogen recombination lines at 5.7 μm, 6.3 μm, 7.5 μm, 11.3 μm, 12.4 μm, 16.2 μm. Top panel shows f_ν against λ to highlight the strong 9.7 μm silicate feature; the final three observations only (Days 529, 591 and 764) have been multiplied by a factor of 10 and offset for clarity. The error bars at 17.5 μm show representative 3σ errors. Bottom panel shows $\log[\lambda f_\lambda]$ against λ; no offsets or other factors in this panel. From Helton et al. (2010). ©AAS. Reproduced with permission.

Table 2: Primary AIR features, and their wavelengths in the ejecta of dusty novae.

λ (μm)	Assignment*	V842 Cen^{†,a,b}	V705 Cas^{c}	DZ Cru^{d}	V2361 Cyg^{e}	V2362 Cyg^{e,f}
3.28	Aromatic C−H stretch	3.28	3.28	—	—	—
3.4	Aliphatic C−H stretch	3.4	3.41	—	—	—
6.2	Aromatic C−C stretch	—	—	6.46	6.37–6.41	6.31–6.36
7.7–8.2	Aromatic C−C stretching bands	7.7	8.06-8.17	8.12	7.96–8.12	7.77–7.90
8.7	Aromatic C−H in-plane bend	8.6	8.7	∘	∘	∘
9.2		∘	9.29	9.26	∘	9.52–9.83
11.5	Aromatic C−H out-of-plane bend	11.3	11.40	10.97	11.37–11.50	11.25–11.40
12.7	C−H out-of-plane bend	12.7	∘	12.36	12.33–12.40	12.46–12.50

*A "∘" indicates that the relevant feature was weak or absent, a "—" that the observations did not cover the relevant wavelength range.

†The wavelengths of the features in papers (a) and (b) were simply reported as the "family of emission features at 3.28, 3.5, 6.2, 7.7, 8.6 and 11.3 μm".

(a): Hyland & McGregor (1989); (b): Smith et al. (1994); (c): Evans et al. (2005); (d): Evans et al. (2010); (e): Helton et al. (2011, 2014); (f) Lynch et al. (2008).

2.4.2. Hydrocarbons

The possibility that hydrocarbon features are present (either from free-flying Polycyclic Aromatic Hydrocarbon (PAH) molecules, or from Hydrogenated Amorphous Carbon (HAC)) was predicted by Mitchell & Evans (1984). These features (to which we shall refer as Aromatic Infrared (AIR) features) have now been detected in several novae, courtesy of their emission at 3.3 μm, 3.4 μm, 6.6 μm, 7.7 μm etc. A selection is shown in Figs. 4, 7 and 8. Note how, in V2362 Cyg, the AIR feature wavelengths and relative fluxes change as the ejecta evolve.

In the majority of astrophysical sources in which they are observed, the main AIR features are seen at (see Allamandola et al., 1989; Tielens, 2008, for comprehensive compilations) 3.29 μm, 3.4 μm, 6.2 μm, 7.6–8.0 μm, 8.7 μm and 11.2 μm, which are attributed to various bend, stretch and wag modes in large PAH molecules (Tielens, 2008).

A list of the more prominent AIR features, and their wavelengths as measured in novae, is given in Table 2, which also gives the assignments. Note that the 9.2 μm feature is not normally recognised as part of the usual "family" of AIR features (see Tielens, 2008), but Ootsubo et al. (2020) (see below) have suggested that it might be attributed to aliphatic hydrocarbons. Minor AIR features, also present in nova spectra, are not listed, but they may appear as "shoulders" on the main features.

The AIR features in novae seem to be unlike those seen in other astrophysical sources, such as planetary nebulae, post-Asymptotic Giant Branch stars, star-forming regions (see Peeters et al., 2002, for a full classification of AIR features in the 6–9 μm wavelength range). In novae the 3.4 μm/3.3 μm flux ratio is large compared with other sources. This may reflect the relative amounts of aromatic and aliphatic hydrocarbons in nova dust, or may indicate the presence of CH_2 and CH_3 groups in silicate grains; laboratory studies (Grishko & Duley, 2002a) have shown that such contaminants enhance the 3.4 μm AIR feature. The lower right panel of Fig. 8 compares nova AIR features with those of Peeters et al.'s "Class C", which Sloan et al. (2007) have attributed to a carrier having predominantly aliphatic bonds.

The AIR feature normally at 7.7 μm appears at 8.2 μm in novae; there are also "shoulder" features (at 8.7 μm and 9.2 μm) on the 8.2 μm feature that may the result of the incorporation of nitrogen-bearing groups into the PAH molecule (Evans et al., 2005). Support for this suggestion comes from the laboratory study by Endo et al. (2021), who found that "Quenched Nitrogen-

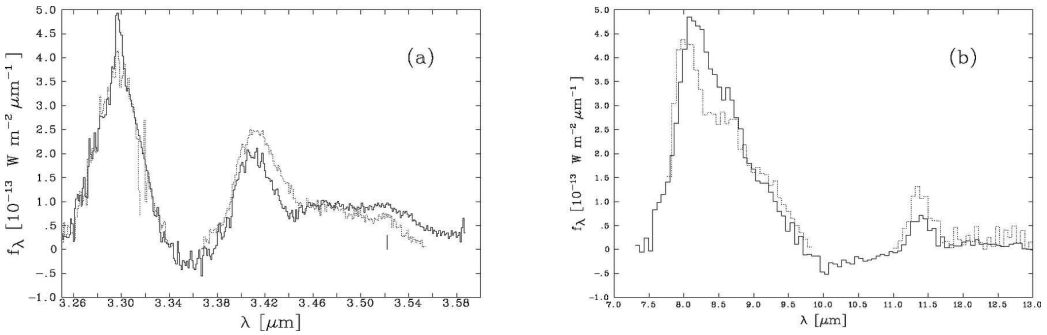


Figure 7: The AIR features in nova V705 Cas. Left: 3 μm band. Note the strength of the 3.4 μm feature relative to that of the 3.28 μm feature. Right: 6–12 μm band. In each case the solid line denotes data from 1994 August (day 253), the dotted line from 1994 October/November (day 320). From Evans et al. (2005). Reproduced with the permission of A. Evans.

included Carbonaceous Composite" (QNCC) reproduces the nova-specific AIR very well. The fact that the nitrogenated PAH molecules 1- and 2-cyanonaphthalene are present in the nearby Taurus Molecular Cloud TMC-1 (McGuire et al., 2021) hints that such compounds must surely have been present in the nascent Solar System.

Furthermore, the 11.25 μm feature in novae appears at longer wavelength (11.4 μm). As the ^{12}C/^{13}C ratio is low in novae, some of these differences may be attributed to isotopic shifts (see Wada et al., 2003). However the wavelength shifts are more likely due to the incorporation of other species such as N into the PAH structure.

2.5. Summary

Classical nova explosions are laboratories in which several important, but poorly understood, astrophysical processes can be observed in real time; in particular they provide the opportunity to observe dust formation. Not only do they produce a variety of grain types, they often form both oxygen- and carbon-rich condensates simultaneously. In principle it is possible to see gas-phase abundances decrease as dust forms and atoms are removed from the gas, although this has been directly observed only in the case of V1370 Aql (Snijders et al., 1987).

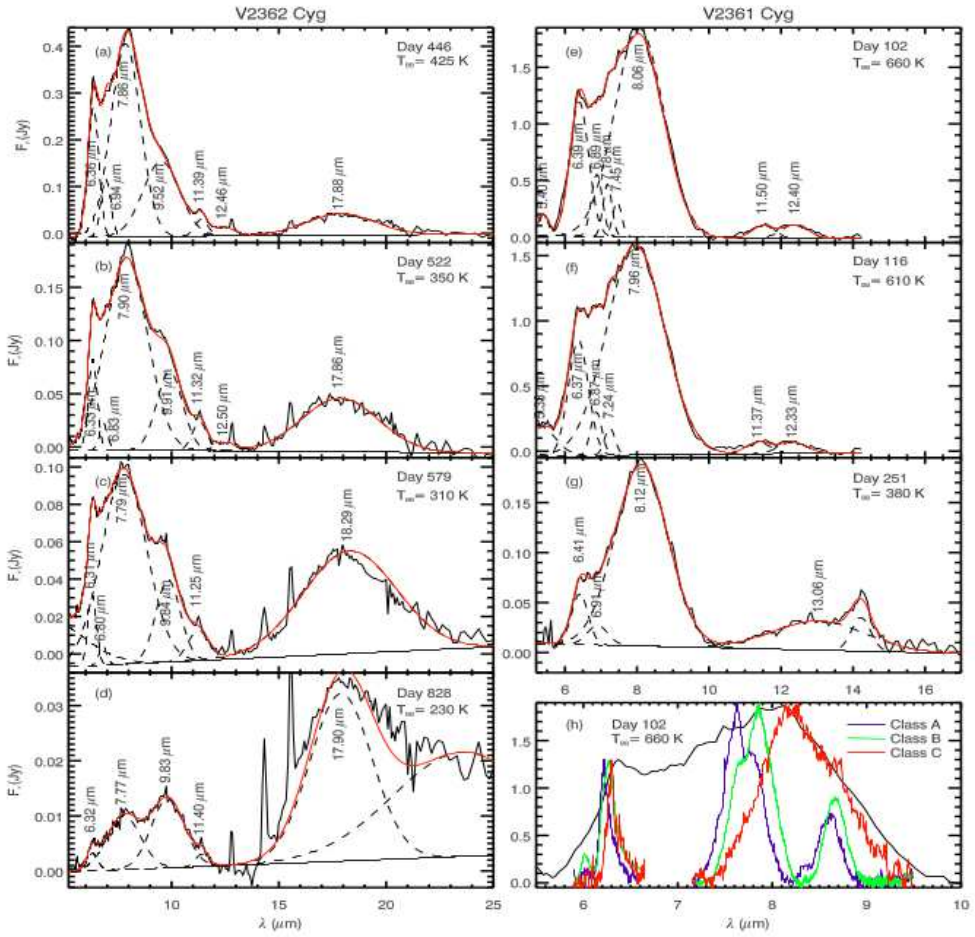


Figure 8: AIR emission in novae V2362 Cyg (left) and V2361 Cyg (right). In both cases a blackbody continuum has been subtracted to highlight the AIR features. In panels (a)–(g) the dashed lines are individual AIR features, fitted with Gaussian components to produce the composite fit (red); peak wavelengths of individual AIR features are indicated (compare with Table 2). Panel (h) shows Class A, B, and C UIR profiles (Peeters et al., 2002) overlayed on the V2361 Cyg spectra from day 102. In V2362 Cyg the features around 9.8 μm and 18 μm are most probably due to silicates. From Helton et al. (2011). ©AAS. Reproduced with permission.

3. "Born-again" giants

3.1. The Very Late Thermal Pulse

It is well known that, when a star evolves away from the Main Sequence (MS), its post-MS evolution depends on its mass. For stars having low to intermediate mass ($\lesssim 8\,M_\odot$; Werner & Herwig, 2006), following the helium core flash, burnout of He occurs in the core on the horizontal branch. It then evolves up the AGB, and the star sheds its outer envelope which remains visible as a planetary nebula (PN), irradiated by the still-hot stellar core. In time the PN disperses and the stellar core becomes a WD.

However, in as many as 10–20% of cases (Blöcker, 2001; Lawlor & MacDonald, 2003), after the star has evolved beyond the post-AGB phase and is evolving towards the WD region, it re-ignites a residual helium shell in a VLTP. It then retraces a large part of its evolutionary track across the Hertzsprung-Russell diagram (Iben, 1982; Herwig, 2001; Lawlor & MacDonald, 2003) and becomes a "Born-Again Giant" (BAG). The final evolution, from pre-WD to the BAG phase, was predicted to take of the order of a few centuries, thus representing a very rapid (and hence seldom seen) phase of stellar evolution.

Whereas several hundred classical novae have been catalogued and studied, both in the Galaxy and in galaxies as far as the Virgo cluster, VLTPs are very rare indeed. Their number is, as of the time of this writing, fewer than ten. These include Sakurai's Object (V4334 Sgr), V605 Aql (Clayton et al., 2013) and FG Sge (Gehrz et al., 2005), although the latter has also been regarded as a Late Thermal Pulse[6] (Jeffery & Schönberner, 2006). Most of these objects are hydrogen-deficient[7], carbon-rich, have extensive dust shells, and each lies at the centre of an old PN. The post-VLTP evolution of Sakurai's Object, FG Sge and V705 Aql have been very similar (Hinkle et al., 2008; Clayton et al., 2006, 2013) and there is a suggestion that they represent different stages along the same evolutionary sequence (Lawlor & MacDonald, 2003).

While it is now understood that they have their origins on the pre-WD core of an AGB star, whether these are isolated objects, or in binary systems, is unclear; the dust disks around V605 Aql (Clayton et al., 2013) and Sakurai's Object (Chesneau et al., 2009) may hint at binarity. Indeed, an

[6]See Werner & Herwig (2006) for the difference between a Late Thermal Pulse and a *Very* Late Thermal Pulse.

[7]However Blöcker & Schönberner (1997) note that FG Sge is not hydrogen deficient.

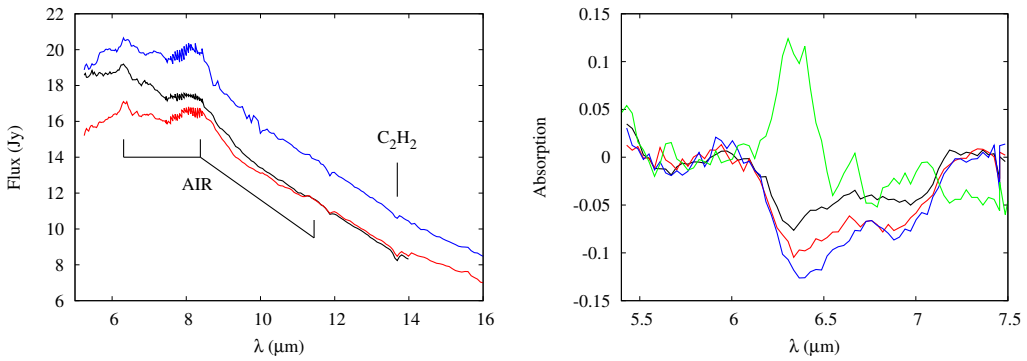


Figure 9: Left panel: Spitzer spectra of FG Sge, showing AIR features and C_2H_2. Right panel: 6.4 μm absorption features in Sakurai's Object, rectified by quadratic continuum (red, blue and black curves denote observations obtained on different dates); green curve is 6.4 μm AIR feature in FG Sge. Evans et al. (in preparation).

alternative interpretation of the phenomenon typified by Sakurai's Object is the rapid accretion of material onto a WD, presumably from a companion (Denissenkov et al., 2017). In such a scenario the flash is recurrent (just as in the case of a nova) and if correct, means that individual objects might make a more substantial contribution to the interstellar medium than is the case for a single, one-off, VLTP.

Detailed modelling by Herwig et al. (2011) and others, based mainly on the behaviour of the well-studied Sakurai's Object, shows that the overall features of VLTPs, such as abundance and isotopic anomalies, can be understood in terms of ingestion of H into the He-shell convection zone. In a short time (typically $\sim$ an hour; Herwig et al., 2011), there occurs a separation of the convection zone into the original zone driven by He-burning, and a new zone driven by the rapid burning of the ingested H. While the process does not have the explosive nature of a nova TNR, it does nevertheless occur on an extremely short time-scale.

Elemental abundances in Sakurai's Object were determined shortly after its VLTP by Asplund et al. (1999). These authors found that, in 1996, it was H-deficient, slightly metal-poor by comparison with solar values, and had a high abundance of some (but not all) *s*-process elements such as Cu, Zr and Y. They concluded that Sakurai's Object had undergone H-burning, followed by He-burning, a second phase of CNO-cycling, and *s*-processing for light s-process elements. The low $^{12}C/^{13}C$ ratio ($\simeq 6$; see e.g., Pavlenko et al., 2004; Worters et al., 2009; Evans et al., 2006, 2020) also points to second stage

CNO-cycling following He-burning. The scheme described by Herwig et al. (2011) results in an over-production of Rb, Sr, and Y (over-abundant relative to solar by $\sim 1.5 - 2$ dex in Sakurai's Object; Asplund et al., 1999) that is two orders of magnitude higher than that of Ba and La (under-abundant relative to solar in Sakurai's Object).

In late 1997 Sakurai's Object ejected a carbon dust shell that completely obscured the central star. At the time of this writing the star remains obscured. The IR SED of Sakurai's Object is almost featureless, and closely resembles a cooling black body with absorption features superimposed (Evans et al., 2020). Assuming that the dust is amorphous carbon, Evans et al. (2020) estimated that the mass of dust resulting from the 1997 ejection event is $\sim 2 \times 10^{-5}\,\mathrm{M}_{\odot}$, although dust ejection did not end with the 1997 event (Evans et al., 2020, 2022). A similar dust mass ($\sim 7 \times 10^{-6}\,\mathrm{M}_{\odot}$) has been determined for V605 Aql (Clayton et al., 2013).

If these dust masses are representative (based of course on *very* small statistics, and see below for FG Sge), then we can make a very crude extimate of the rate at which VLTPs inject dust into the interstellar medium. The formation rates for planetary nebulae ($\sim 4.4 \times 10^{-3}$ kpc^{-3} yr^{-1}) and white dwarfs ($\sim 2 \times 10^{-3}$ kpc^{-3} yr^{-1}) are very similar (Phillips, 1984). Taking 3×10^{-3} kpc^{-3} yr^{-1}, and assuming that 15% of these stellar deaths undergo a VLTP, ejecting $10^{-5}\,\mathrm{M}_{\odot}$ of amorphous carbon dust, then $\sim 4.5 \times 10^{-9}\,\mathrm{M}_{\odot}$ of carbon dust is injected kpc^{-3} yr^{-1}.

The smooth dust SED of Sakurai's Object is in distinct contrast to the IR SED of FG Sge, which shows the AIR features at 6.4 μm, 8 μm and (weakly) 11.5 μm (see Fig. 9). Although Sakurai's Object has (as of the time of this writing) shown no evidence of AIR emission, Evans et al. (2020) noted weak absorption features around 6–7 μm, which they attributed to nitrogenated HAC. Similar features are often seen in lines of sight through molecular clouds and environments containing young stellar objects (Boogert et al., 2008). The temperature of the dust shell around FG Sge is roughly constant in time ($\sim 800 - 1000$ K; Gehrz et al., 2005), and the dust mass is $\sim 6.8 \times 10^{-9}\,\mathrm{M}_{\odot}$.

The 6.4 μm feature profiles in Sakurai's Object, which in Evans et al. had been obtained by rectifying with respect to a black body, were rather ill-defined. Rectifying with respect to the adjacent continuum brings the features out rather better (see Fig. 9); these absorption features in Sakurai's Object seem to correspond well with the AIR emission features in FG Sge (see Fig. 9). A detailed analysis of these features by Bowey (2021) identifies them

with a mix of PAHs, melilite, and large ($\sim 20\,\mu$m) SiC grains. Interestingly, melilite is a crystalline silicate that is a significant component of calcium-aluminium-rich inclusions in primitive meteorites and Bowey (2021) suggests that the melilite in the winds of objects like Sakurai's Object may be a precursor to meteoritic melilite. However it is likely that the melilite in calcium-aluminium-rich inclusions condensed in the early Solar System.

Laboratory work by Grishko & Duley (2002b), in which they carried out laser ablation of graphite in H_2/N_2 and NH_3 gas mixtures, showed that the resulting material showed features in the 6.0–6.5 μm range. Given that Asplund et al. (1999) had found that, before it was enshrouded by the dust, nitrogen was overabundant in Sakurai's Object, nitrogenation of the AIR carrier may be at work in Sakurai's Object and FG Sge, as it might have been in the case of novae (see Section 2.4.2 above).

3.2. Summary

What is known about dust in VLTPs relies heavily on observations of Sakurai's Object and, to a lesser extent FG Sge and V605 Aql. Nevertheless enough information has been garnered over the past few years to enable the possible identification of VLTP dust in material that may have been ingested into the early Solar System.

4. The pre-solar connection

Stardust in the primitive solar nebula suffered a large amount of destructive processing since the individual dust grains migrated from their various stellar origins, via the formation of the Sun and planets, to the present day. The result is that precious few of the "pristine" stellar grains remain. However, despite the fact that recovered material is usually a heterogeneous mix of grains having a variety of stellar origins, laboratory analysis of cometary materials, meteorites, and IDPs believed to have been released from comet nuclei can reveal information about the stellar sources of their constituent dust particles.

In attempting to identify grains that originated in novae and VLTPs in pre-solar material, we should be mindful of the potential ambiguities. For example, did SiC form in the ejecta of novae or in those of Type II supernovae (Nittler & Hoppe, 2004a,b; Liu et al., 2016)? And isotopic ratios, unless several are available (see, e.g., Iliadis et al., 2018), may not unambiguously point to an origin in novae, VLTPs or supernovae. Furthermore, nova and VLTP

grains in (for example) IDPs have to be separated from the overwhelming amount of minerals that are of solar, and other stellar, origin.

4.1. Novae

Evidence for a nova origin for some pre-solar grains comes therefore from studies of pre-solar grains identified in meteorites and of IDPs recovered from comet tails (Messenger, 2002).

The most decisive connection between nova grains and pre-solar material is the close similarity in the isotopic ratios found in certain cometary grains and the predictions of the TNR scenario. As noted in Section 2.2, the TNR imprints nova-specific isotope ratios, e.g. $^{12}C/^{13}C$, $^{14}N/^{15}N$, $^{20}Ne/^{22}Ne$ on the nova ejecta. Bose & Starrfield (2019) compared isotope ratios for ejecta produced in CO nova TNR models with isotope ratios observed in thirty pre-solar grains from meteorites and found evidence for pure CO nova ejecta material in five of them. They suggested that these SiC grains formed in the winds of CO novae. Furthermore, Bose & Starrfield (2019) found that the elemental and isotopic abundances in one pre-solar grain matched the prediction of TNR modelling, without the need for dilution. Iliadis et al. (2018) identified six pre-solar grains having isotopic signatures that indicated a "high plausibility" that they originated in a CO nova, without assuming any dilution of the ejecta before grain condensation. Additional studies by Haenecour et al. (2019) and by Leitner and Hoppe (2019) confirm the ability to discern grains in primitive Solar System materials that were produced in nova events.

Analysis of neon isotope abundances in fragmets of IDPs collected by a U2 aircraft from comet orbital trails suggests that TNRs from nova explosions on ONe WDs may also have produced some of the stellar debris that was present in the primitive Solar System (Pepin et al., 2011). Pepin et al. identified two distinct categories of IDPs having cometary origin: those (designated "normal") having a $^{20}Ne/^{22}Ne$ ratio (=13.9) and He content that is characteristic of the solar wind, and those (designated "anomalous") with no detectable solar wind He and a ^{22}Ne abundance that is essentially uniform, with $^{20}Ne/^{22}Ne$ ratios ranging from $\sim$ 26 to $\sim$ 153 (see Fig. 10). In none of the anomalous IDPs was He detected, clearly illustrating that these are a distinct population, distingiushable from IDPs that have had extended exposure to the solar wind.

By comparing the He and Ne isotopic ratios found in the anomalous IDPs with those predicted for ONe novae and core collapse supernovae, Pepin et al.

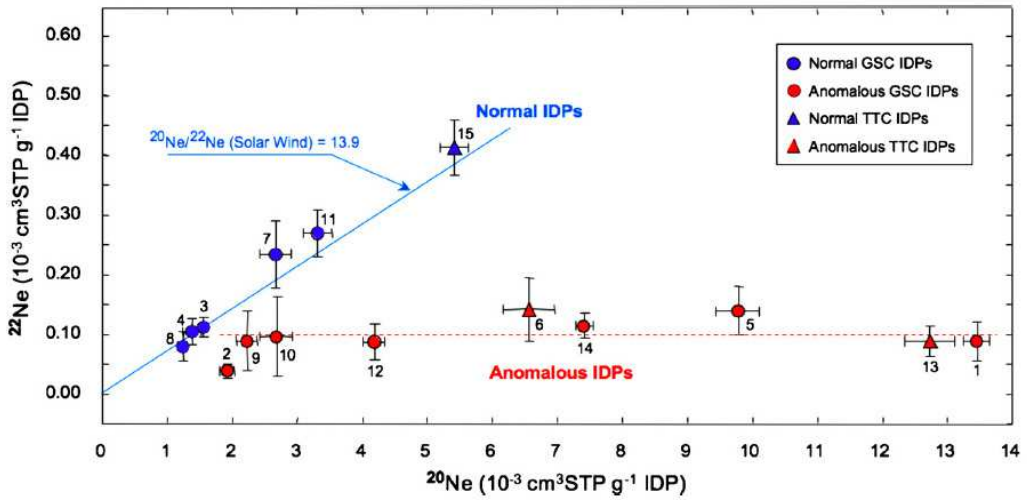


Figure 10: Concentrations of ^{20}Ne and ^{22}Ne in 15 IDPs from the Grigg-Skjellerup (GSC) and Tempel-Tuttle (TTC) cometary collections, where 1 cm^3 STP contains 2.69×10^{19} Numbering of points corresponds to the IDP numbering in Table 1 of Pepin et al. (2011). Normal IDPs show abundances expected for long-term exposure to the solar wind, as would be expected for asteroidal particles (blue symbols and line). Error bars are 1σ. Details of the analysis are given in Pepin et al. (2011). Figure from Pepin et al. (2011). ©AAS. Reproduced with permission.

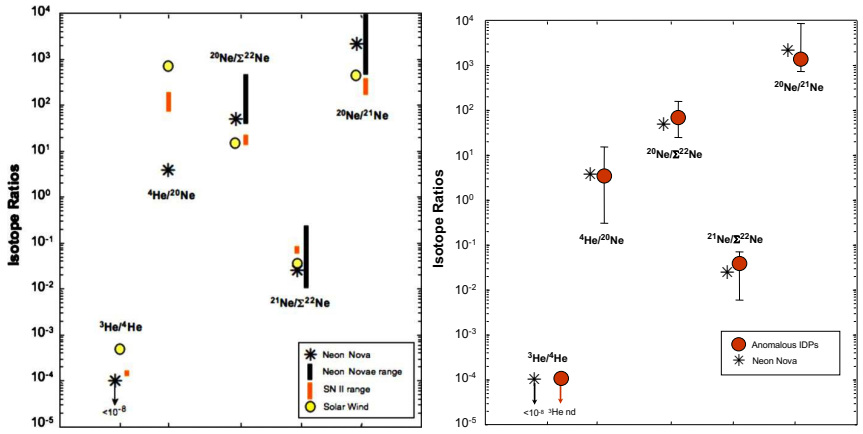


Figure 11: Left panel: Modelled He and Ne isotope ratios in neon nova ejecta, with core collapse supernova models and solar wind ratios plotted for comparison. The vertical black bars indicate the ranges of ratios generated in models of neon nova outbursts over a WD mass range of 1.00–1.35 $M_\odot$ with several different choices for initial compositions and nuclear reaction networks (José et al., 2004). The neon nova ejecta compositions for a 1.25 $M_\odot$ ONe WD are shown by the star symbols. Σ^{22}Ne represents the sum of the ^{22}Ne and the β^+-active ^{22}Na synthesized in the TNR. Orange bars are compositional ranges for the total ejecta from models of nucleosynthesis in Type II supernovae (SNe II) of 15 and 25 $M_\odot$ (see Rauscher et al., 2002). Right panel: Measured He and Ne isotope ratios in the anomalous IDPs analyzed by Pepin et al. (2011) compared with solar wind compositions and TNR modeling results. The IDP Data points are average ratios in the anomalous groups; thin vertical bars indicate minimum and maximum measured values. "nd" indicates not detected. Neon nova modeling results for a 1.25 $M_\odot$ ONe WD are shown by the star symbols. Left panel from Pepin et al. (2011); right panel is a modified version of a figure from Pepin et al. (2011) provided by R. O. Pepin. ©AAS. Reproduced with permission.

(2011) argued that several of the anomalous IDPs have He and Ne isotope ratios that are consistent with their having been condensed in the outflow of a neon nova (see Fig. 11).

There is some evidence that nova dust in meteorites may have originated in the ejecta of novae that originated on both CO and ONe WD. Gyngard et al. (2010) have determined isotopic ratios for O and Mg in grains recovered from the Murray carbonaceous chondrite meteorite, and find that large excesses of ^{17}O, ^{25}Mg and ^{26}Mg point to an origin in a TNR on a CO WD. Starrfield et al. (1997) have argued that the class of ONe novae may form dust grains that carry the Ne-E (Black & Pepin, 1969) and ^{26}Mg (Gray & Compston, 1974) anomalies observed in meteoritic grains.

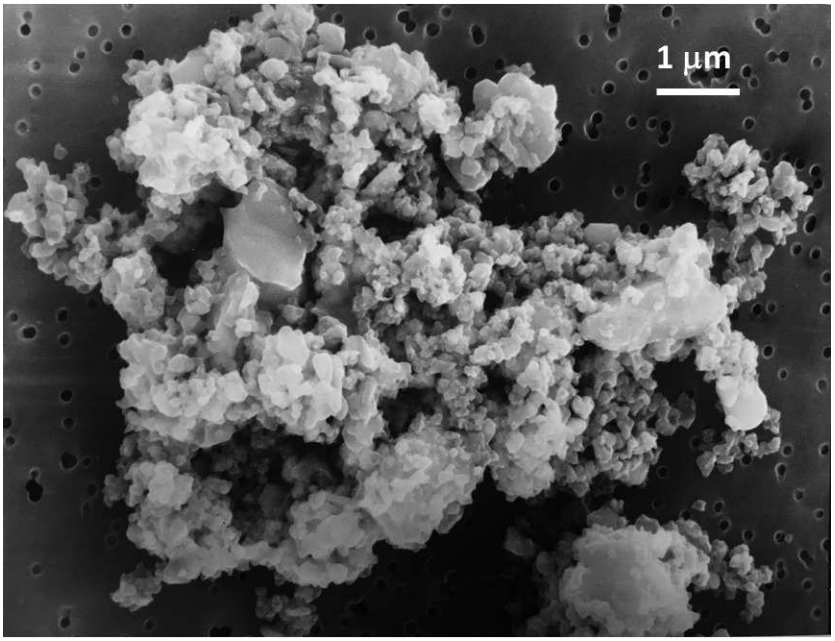


Figure 12: Electron microscope image of an 18 μm long IDP, possibly of cometary origin, collected by a NASA high-altitude research aircraft. It is a porous aggregate of unequilibrated components that were never compacted by mechanical force, heating or aqueous alteration. It has the elemental composition of a carbonaceous chondrite but a totally different structure. This type of aggregate structure is likely to be characteristic of micron and larger circumstellar grains that accrete by gentle processes and not altered after formation. Image and caption courtesy of D. E. Brownlee.

Far more tentative connections between nova dust and IDPs are in the size distribution of the particles, and in the presence of AIR emission. The small grains in subclusters in some IDPs (see Fig. 12) and in comets (see Fig. 13, in which "superheat" is the ratio of the grain temperature and the temperature a blackbody would have at the comet's heliocentric distance; see Gehrz & Ney (1992) for a discussion) have the same 0.1 μm to 0.7 μm size range as the grains that grow in nova outflows (see, e.g., Shore et al., 1994; Helton et al., 2010; Gehrz et al., 2018). However, the size distribution is a poor discriminant, as the presence of particles of this size are inferred in the outflows of evolved stars (see, e.g., Höfner & Olofsson, 2018, and references therein) and in particular, in the ejecta of the VLTP Sakurai's Object (Tyne et al., 2002).

In common with a large variety of astrophysical sources, some novae, and

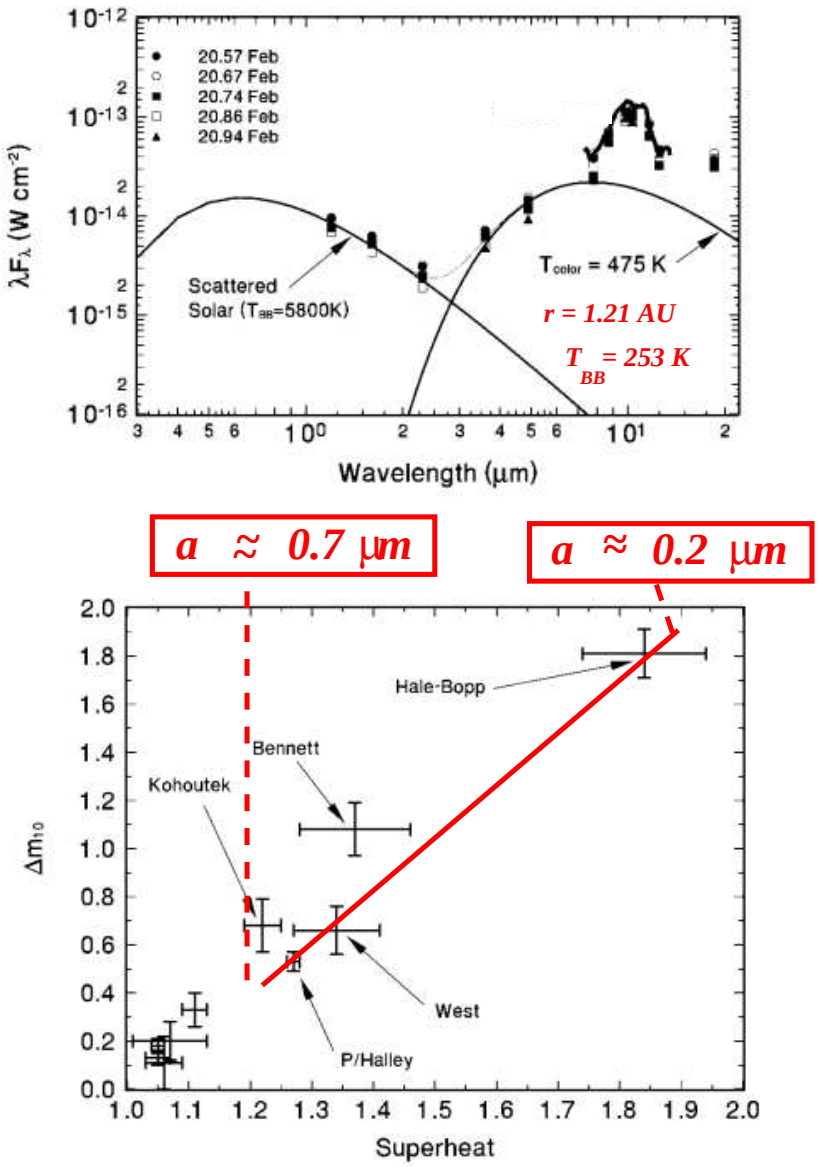


Figure 13: Top panel: Infrared SED of Comet Hale–Bopp (C/1995 O1) showing a superheat (see text) of 1.21 and a 10 μm silicate feature strength of 1.8 magnitudes, indicating an average grain radius of 0.2 μm. Bottom panel: Superheat and 10 μm silicate feature strength plotted from a sample of eight comets showing that comet grains have been observed to span a range of 0.2 μm to 0.7 μm in radius. Nova grains span the same radius range. Figure after Williams et al. (1997). ©AAS. Reproduced with permission.

some comets, display AIR emission. As noted above (Section 2.4.2), those seen in novae (Evans et al., 2005, 2010; Helton et al., 2011, 2014) differ significantly from those seen in other sources, possibly due to the incorporation of nitrogen and/or nitrogen groups into the AIR carrier (Evans et al., 2005).

The presence of AIR features in comets has been claimed in the Infrared Space Observatory (Kessler et al., 1996) spectrum of C/1995 O1 (Hale-Bopp) (Lisse et al., 2007), although these findings proved to be controversial (Crovisier & Bockelée-Morvan, 2008; Lisse, 2008). The detection of AIR features in *Spitzer* IRS spectra of the debris from comet 9P/Tempel 1 following the Deep Impact event (Lisse et al., 2006, 2007) is less contentious, although these features resemble the "conventional" family of features rather than those seen in novae.

On the other hand, AIR features with peak wavelengths close to those in novae V705 Cas and DZ Cru have been reported in the spectrum of comet 21P/Giacobini-Zinner (Ootsubo et al., 2020) (see Fig. 14). The residuals in the 6–12 μm range, after removing the contibution of silicates and other components, revealed apparent features at 8.236 μm, 8.475 μm, 9.229 μm and 11.108 μm, which match the AIR features in novae (see Table 2). While these features were not detected in a *Spitzer* IRS observation (Kelley et al., 2021), the Ootsubo et al. and *Spitzer* data were separated in time by about 5 months. Clearly there were differences in the modes of observation but more significantly, there were large differences in the heliocentric distance (and hence cometary environment) between the two observations. With the exception of the silicate features, the *Spitzer* IRS spectrum is feature-free for $\lambda < 14\,\mu$m (M. S. P. Kelley, personal communication), so the jury is out on the presence of AIR features in the spectrum of 21P/Giacobini-Zinner. Clearly further observations are required to resolve this issue.

4.2. Born-Again Giants

Connections of VLTP dust to pre-solar grains is rather sparse by comparison with novae, and relies entirely on isotopic ratios for species that are likely to have been overproduced in the VLTP. In view of the comparatively recent (compared with novae) impetus in studing the nuclear networks in VLTPs there is little that can be said at this stage, and much of the evidence is based on advancements since the VLTP of Sakurai's Object.

Jadhav et al. (2013) have shown that the Ca and Ti isotopic anomalies in high density pre-solar graphite grains of the Orgueil meteorite, combined with their low $^{12}C/^{13}C$ ratio, tally well with predictions of the H-ingestion

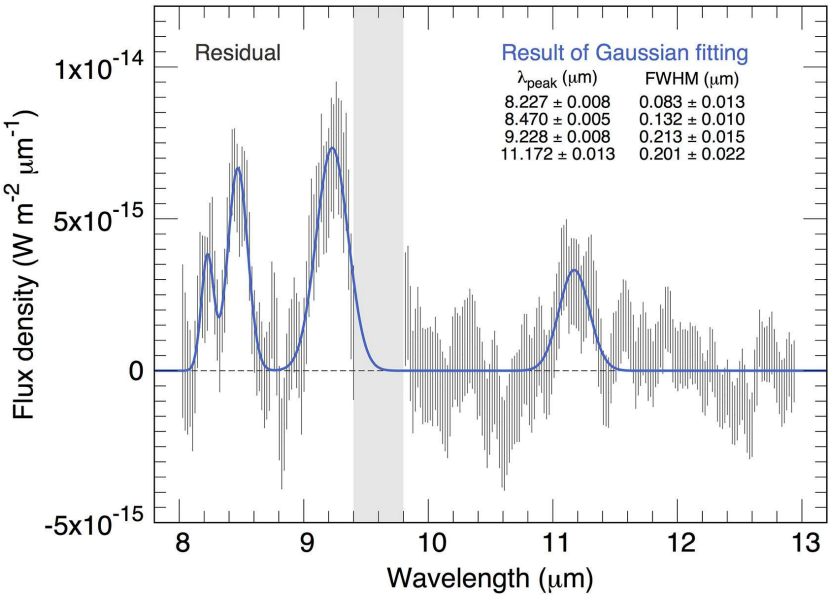


Figure 14: Possible 6–12 μm AIR features in comet 21P/Giacobini-Zinner. From Ootsubo et al. (2020). Figure reproduced with the permission of T. Ootsubo.

phase during a VLTP event in post-AGB stars (Herwig et al., 2011). The Herwig et al. calculations were informed by the photospheric abundances in Sakurai's Object as determined by Asplund et al. (1999) before it disappeared from view. In Fig. 15 are plotted the ratios, as δ-values, i.e. deviations from the terrestrial ratios, in permil (‰); this figure also includes some predicted ratios for the envelopes of low-metallicity AGB stars. It is evident that the high Ca isotopic anomalies measured in Orgueil are not consistent with standard AGB models, and point to an origin in a VLTP, which can account for the large Ca and Ti anomalies observed in grains with low $^{12}C/^{13}C$ ratios. Amari et al. (2001) proposed born-again AGB stars as one of the stellar sources of SiC AB grains defined as having $^{12}C/^{13}C$ ratios < 10. Fujiya et al. (2013) have also argued that the C, Si and S isotope measurements in SiC grains of Type AB are consistent with an origin in a VLTP, but they caution that uncertainties in VLTP models mean that a definitive conclusion is not possible.

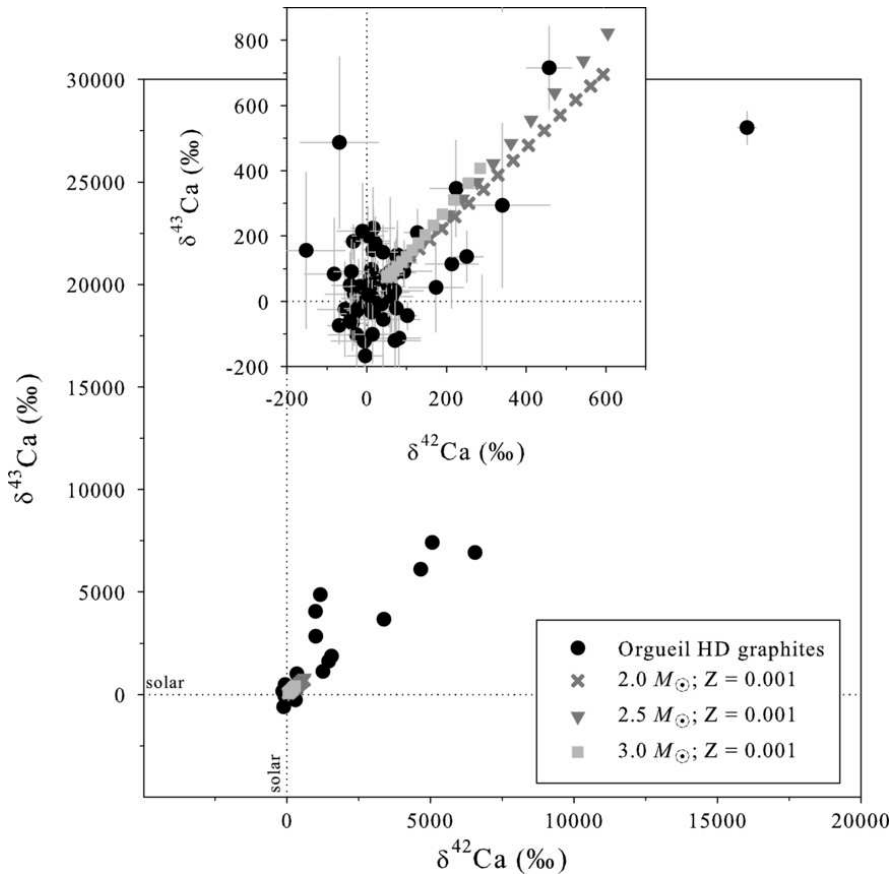


Figure 15: Three-isotope plot of ^{42,43}Ca/^{40}Ca isotopic ratios measured in Orgueil. Black dots are Orgueil data, the crosses, inverted triangles and squares are for low metallicity AGB stars. The δ values are deviations from terrestrial ratios, in permil (‰). Error bars are 1σ. Dashed lines indicate solar ratios. Figure from Jadhav et al. (2013). ©AAS. Reproduced with permission.

5. Some speculative (and provocative) concluding remarks

Despite that fact that novae (and to a lesser extent, VLTPs) are not expected to be major contributors to the Galactic interstellar dust population (see, e.g., Table 1 in Gehrz, 1989), it is gratifying that there is ample evidence that dust from these sources has survived, and has been identified in primitive meteorites and IDPs.

Both novae and VLTPs, by virtue of their C-enriched ejecta, contain an abundance of organic material, as evidenced by (novae), HCN, C_2H_2 and polyynes (Sakurai's Object), and both types of object display AIR features. This is of course a trait that they share with the detritus of other low-mass stars as they approach the stellar graveyard.

The nova and VLTP dust would almost certainly have transported with them the organic material they contain. The similarity of the organics observed in novae and in VLTPs (and other sources of stardust) with material present in the current Solar System must surely beg the question: what role might these organic materials have played in the origin and evolution of pre-biotic material in the early Solar System, and in the emergence of primitive biota on the early Earth? For example, Ootsubo et al. (2020) (amongst many others) have suggested that comets aggregated and grew in the solar nebula, and that cometary nuclei formed in the primitive solar nebula could have delivered pre-biotic organic molecules to the infant Earth via impacts.

Organic material is of course widespread in the Solar System, the interstellar medium and beyond (see, e.g., Kwok, 2016, for a very comprehensive review). Many molecules detected in astrophysical environments are precursors to the molecules that are essential for life. For example, Hadraoui et al. (2019) reported the episodic detection of glycine (the simplest amino acid and, like the components of deoxyribonucleic acid (DNA), a nitrogenated/oxygenated hydrocarbon) in comet 67P/Churyumov-Gerasimenko, while a glycine precursor has been detected in several molecular clouds (Suzuki et al., 2016). The possibility of detecting glycine itself in proto-planetary systems has been discussed by Jiménez-Serra et al. (2014).

As is well-known, DNA – the cornerstone of all life on Earth – consists of four nucleotides[8] linked by phosphodiester bonds. An intriguing considera-

[8]The "ACGT" sequence known to anyone who has studied their ancestry: Adenine (a nitrogenated hydrocarbon), Cytosine, Guanine and Thymine (nitrogenated/oxygenated hydrocarbons).

tion is that, whereas hydrocarbons are commonplace in astrophysical environments, hydrocarbons that formed in environments (like novae and VLTPs) in *which C, N, O and P are overabundant* might be particularly relevant. The ingredients for DNA were cooked in nova and (to a lesser extent) VLTP events.

Putting aside the issue of isotopic abundances, do we owe our very existence to dust from novae and VLTPs that was ingested into the proto-solar nebula?

Acknowledgements

We thank Sachiko Amari, Don Brownlee, Jordi José, Mike Kelley, Arumugam Mahendrasingam, Bob Pepin, Sumner Starrfield and Chick Woodward for their helpful comments on, and input into, earlier versions of this chapter. We also thank the various authors and publishers for permission to reproduce figures from the literature.

RDG was supported for observations presented herein by the National Science Foundation, NASA and the United States Air Force.

References

Allamandola L. J., Tielens A. G. G. M. and Barker J. R. (1989) Interstellar Polycyclic Aromatic Hydrocarbons: the infrared emission bands, the excitation/emission mechanism, and the astrophysical implications. *ApJS*, **71**, 733-775

Amari S., Nittler L. R., Zinner E., Lodders K. and Lewis R. S. (2001) Presolar SiC Grains of Type A and B: their isotopic compositions and stellar origins. *ApJ.* **559**, 463-483

Anders E. and Grevesse N. (1989) Abundances of the elements: meteoritic and solar. *Geochim. Cosmochim. Acta*, **53**, 197-214.

Asplund M., Lambert D. L. Kipper T., Pollacco D. and Shetrone M. D. (1999) The rapid evolution of the born-again giant Sakurai's object. *A&A*, **343**, 507-518.

Asplund M., Grevesse, N., Sauval A. J. and Scott P. (2009) The chemical composition of the Sun. *ARA&A*, **47**, 481-522.

Banerjee D. P. K. and Ashok N. M. (2012) Near-infrared properties of classical novae: a perspective gained from Mount Abu Infrared Observatory. *BASI*, **40**, 243-265.

Banerjee D. P. K., Strivastava M. K., Ashok N. M. and Venkataraman V. (2016) Near-infrared studies of the carbon monoxide and dust-forming Nova V5668 Sgr. *MNRAS*, **455**, L109-L113.

Banerjee D. P. K., Woodward C. E., Joshi V., Evans A.,Walter F. M., Marion G. H., Hsiao E. Y., Ashok N. M., Gehrz R. D. and Starrfield S. (2023) Snowflakes in a Furnace: Formation of CO and Dust in a Recurrent Nova Eruption. *ApJL*, **954**, L16(6pp)

Bath G. T. and Shaviv G. (1976) Classical novae – a steady state, constant luminosity, continuous ejection model. *MNRAS*, **175**, 305-322.

Black D. C. and Pepin R. O. (1969) Trapped neon in meteorites – II. *Earth & Planetary Sciences*, **6**, 395-405.

Blöcker T. (2001) Evolution on the AGB and beyond: on the formation of H-deficient post-AGB stars. *Ap&SpSci*, **275**, 1-14.

Blöcker T. and Schönberner D. (1997) Stellar evolution of low and intermediate-mass stars. III. an application of evolutionary post-AGB models: the variable central star FG Sagittae. *A&A*, **324**, 991-997.

Bode, M. F., Evans, A., Whittet D. C. B., Aitken D. K., Roche P. F. Anderegg Whitmore, B. (1984) Infrared photometry and spectrophotometry of Nova Aquilae 1982. *MNRAS*, **207**, 897-907

Bode M. F. and Evans A. (2008) *Classical Novae*, (eds. M. F. Bode and A. Evans), second edition, Cambridge University Press, Cambridge.

Boogert, A. C. A., Pontoppidan K. M., Knez C., Lahuis F., Kessler-Silacci J., van Dishoeck E. F., Blake G. A., Augereau J.-C., Bisschop S. E., Bottinelli S., Brooke T. Y., Brown, J., Crapsi A., Evans N. J., Fraser H. J., Geers V., Huard T. L., Jørgensen J. K., Öberg K. I., Allen L. E., Harvey P. M., Koerner D. W., Mundy L. G., Padgett D. L., Sargent A. I. and Stapelfeldt K. R. (2008) The c2d Spitzer spectroscopic survey of ices around low-mass Young Stellar Objects. I. H_2O and the 5-8 μm Bands. *ApJ*, **678**, 985-1004.

Bose, M. and Starrfield, S. (2019) Condensation of SiC Stardust in CO Nova Outbursts. *ApJ*, **873**, 14-24.

Bowey J.E. (2021) Dust changes in Sakurai's Object: new PAHs and SiC withcoagulation of submicron-sized silicate dust into 10 μm-sized melilite grains *MNRAS*, **505**, 568-581.

Brown A. G. A., et al. (2020) Gaia Early Data Release 3: Summary of the contents and survey properties *A&A*, Special Issue on Gaia Early Data Release 3, arXiv:2012.01533

Chesneau O., Clayton G. C., Lykou F., De Marco O., Hummel C. A., Kerber F., Lagadec E., Nordhaus J., Zijlstra A. A. and Evans, A. (2009) A dense disk of dust around the born-again Sakurai's object. *A&A*, **493**, L17-L20.

Chesneau O., Lagadec E., Otulakowska-Hypka M., Banerjee D. P. K., Woodward C. E., Harvey E., Spang A., Kervella P., Millour F., Nardetto N., Ashok N. M., Barlow M. J., Bode M. F., Evans A., Lynch D. K., O'Brien T. J., Rudy R. J. and Russell R. W. (2012) The expanding dusty bipolar nebula around the nova V1280 Scorpi. *A&A*, **545**, A63-A72.

Clayton D. D. and Wickramasinghe N. C. (1974) On the development of infrared radiation from an expanding nova shell. *Ap&SpSci*, **42**, 463-475.

Clayton G. C., Kerber F., Pirzka, N., De Marco O., Crowther P. A. and Fedrow J. M. (2006) V605 Aquilae: The older twin of Sakurai's Object. *ApJL*, **646**, L69-L72.

Clayton G. C. (2012) What are the R Coronae Borealis stars? *JAAVSO*, **40**, 539.

Clayton G. C., Bond H. E., Long L. A., Meyer P. I., Sugerman B. E. K., Montiel E., Sparks W. B., Meakes M. G., Chesneau O. and De Marco O. (2013) Evolution of the 1919 ejecta of V605 Aquilae. *ApJ*, **771**, 130(10pp).

Crovisier J. and Bockelée-Morvan D. (2008) Comment on "Comparison of the composition of the Tempel 1 ejecta to the dust in Comet C/Hale Bopp 1995 O1 and YSO HD 100546" by C.M. Lisse, K.E. Kraemer, J.A. Nuth III, A. Li, D. Joswiak. *Icarus*, **195**, 938-940.

De K., Kasliwal M. M., Hankins M. J., Sokoloski J. L., Adams S. M., Ashley M. C. B., Babul A.-N., Bagdasaryan A., Delacroix A., Dekany R., Greffe T., Hale D., Jencson J. E., Karambelkar V. R., Lau R. M., Mahabal A., McKenna D., Moore A. M., Ofek E. O., Sharma M., Smith R. M., Soon J., Soria R., Srinivasaragavan G., Tinyanont S., Travouillon T., Tzanidakis A. and Yao Yuhan (2021) A population of heavily reddened, optically missed novae from Palomar Gattini-IR: Constraints on the Galactic nova rate. *ApJ*, **912**, 19(20pp)

Denissenkov P. A., Herwig F., Battino U., Ritter C., Pignatari M., Jones S. and Paxton B. (2017) I-process Nucleosynthesis and Mass Retention Efficiency in He-shell Flash Evolution of Rapidly Accreting White Dwarfs. *ApJL*, **834**, L10(5pp)

Derdzinski A. M., Metzger B. D. and Lazzati D. (2017) Radiative shocks create environments for dust formation in classical novae. *MNRAS*, **469**, 1314-1329.

Endo, I., Sakon I., Onaka T., Kimura Y., Kimura S., Wada S., Helton, L. A., Lau R. M., Kebukawa Y., Muramatsu Y., Ogawa N. O., Ohkouchi N., Nakamura M. and Kwok, S. (2021) On the Nature of Organic Dust in Novae. *ApJ*, **917**, 103 (10pp).

Evans A., Geballe T. R., Rawlings J. M. C., Eyres S. P. S. and Davies J. K. (1997) Infrared spectroscopy of Nova Cassiopeiae 1993. II. Evolution of the dust. *MNRAS*, **292**, 192-204.

Evans A., Tyne V. H., Smith O., Geballe T. R., Rawlings J. M. C. and Eyres S. P. S. (2005) Infrared spectroscopy of Nova Cassiopeiae 1993. IV. A closer look at the dust. *MNRAS*, **360**, 1483-1492.

Evans A., Tyne V. H., van Loon J. Th., Smalley B., Geballe T. R., Gehrz R. D., Woodward C. E., Zijlstra A. A., Polomski E., Rushton M. T., Eyres S. P. S., Starrfield S., Krautter J. and Wagner R. M. (2006) The Spitzer Infrared Spectrometer view of V4334 Sgr (Sakurai?s Object). *MNRAS*, **373**, L75-L79.

Evans A., Woodward C. E., Helton L. A., van Loon J. Th., Barry R. K., Bode M. F., Davis R. J., Drake J. J., Eyres S. P. S., Geballe T. R., Gehrz R. D., Kerr T., Krautter J., Lynch D. K., Ness J.-U., O'Brien T. J., Osborne

J. P., Page K. L., Rudy R. J., Russell R. W., Schwarz G., Starrfield S. and Tyne V. H. (2007) Silicate dust in the environment of RS Ophiuchi following the 2006 eruption. *ApJL*, **671**, L157-L160.

Evans A., Gehrz R. D., Woodward C. E., Helton L. A., Rushton M. T., Bode M. F., Krautter J., Lyke J., Lynch D. K., Ness J.-U., Starrfield S., Truran J. W. and Wagner R. M. (2010) The peculiar dust shell of Nova DZ Cru (2003). *MNRAS*, **406**, L85-L89.

Evans A. and Gehrz R. D. (2012) Infrared emission from novae. *BASI*, **40**, 213-241.

Evans A. and Rawlings J. M. C. (2008) Dust and molecules in nova environments. In *Classical Novae* (eds. M. F. Bode and A. Evans), Cambridge University Press, Cambridge, Chapter 13, 308-334

Evans A., Bode M. F., O'Brien T. J. and Darnley M. J. (2008) RS Ophiuchi (2006) and the Recurrent Nova Phenomenon, Astronomical Society of the Pacific Conference Series, volume **409**, San Francisco

Evans A., Banerjee D. P. K., Gehrz R. D., Joshi V., Ashok N. M., Ribeiro V. A. R. M., Darnley M. J., Woodward C. E., Sand D., Marion G. H., Diamond T. R., Eyres S. P. S., Wagner R. M., Helton L. A., Starrfield S., Shenoy D. P., Krautter J., Vacca, W. D. and Rushton M. T. (2017) Rise and fall of the dust shell of the classical nova V339 Delphini. *MNRAS*, **466**, 4221-4238

Evans A., Gehrz R. D., Woodward C. E., Banerjee D. P. K., Geballe T. R., Clayton G. C., Sarre P. J., Starrfield S., Hinkle K., Joyce R. R., Lykou F., Helton L. A., Eyres S. P. S., Worters H., Montiel E. J., Liimets T., Zijlstra A., Richter M. and Krautter J. (2020) The infrared view of dust and molecules around V4334 Sgr (Sakurai's object): a 20-yr retrospective. *MNRAS*, **493**, 1277-1291.

Evans A., Banerjee D. P. K., Geballe T. R., Gehrz R. D., Woodward C. E., Hinkle K., Joyce R. R., and Shahbandeh M. (2022) V4334 Sgr (Sakurai's Object): still churning out the dust. *MNRAS*, **511**, 713-722.

Ferland G. J. and Shields G. A. (1978a) Fine-structure lines and the 10 micron excess of Nova Cygni 1975. *ApJL*, **224**, L15-L18

Ferland G. J. and Shields G. A. (1978b) Heavy element abundances of Nova Cygni 1975. *ApJ*, **226**, 172-185.

Ferland G. J., Chatzikos M., Guzmán F., Lykins M. L., van Hoof P. A. M., Williams R. J. R., Abel N. P., Badnell N. R., Keenan F. P., Porter R. L. and Stancil P. C. (2017) The 2017 Release Cloudy. *Rev. Mex. Astronomía Astrofísica*, **53**, 385-438.

Fujiya W., Hoppe P., Zinner E., Pignatari M. and Herwig F. (2013) Evidence for radiogenic sulfur-32 in Type AB presolar silicon sarbide grains? *ApJL*, **776**, L29(6pp).

Fujii M., Arai A. and Kawakita H. (2021) Transient formation of C_2 and CN in the near-maximum phase of Nova Cas 2020 (=V1391 Cas) *ApJ*, **907**, 70(4pp)

Gallagher J. S. and Starrfield S. (1976) On the total energy output of the nova outburst *MNRAS*, **176**, 53-61

Gehrz R. D., Grasdalen G. L., Hackwell J. A. and Ney E. P. (1980a) The evolution of the dust shell of Nova Ser 1978 *ApJ*, **237**, 855-865.

Gehrz R. D., Hackwell J. A., Grasdalen G. I., Ney E. P., Neugebauer G. and Sellgren K. (1980b) The optically thin dust shell of Nova Cyg 1978. *ApJ*, **239**, 570-580.

Gehrz R. D., Grasdalen G. L., Greenhouse M., Hackwell J. A., Hayward T. and Bentley A. F. (1986) The neon nova. II. Condensation of silicate grains in the ejecta of Nova Vulpeculae 1984 number 2. *ApJ*, **308**, L63-66.

Gehrz R. D. (1989) Sources of stardust in the Galaxy. In "Interstellar Dust", proceedings of IAU Symposium 135, eds L. J. Allamandola, A. G. G. M. Tielens, Kluwer Academic Publishers, Dordrecht, The Netherlands, 445-453.

Gehrz R.D. and Ney E. P. (1992) 0.7- to 23- μm photometric observations of P/Halley 1986 III and six recent bright comets. *Icarus*, **100**, 162-186

Gehrz R. D., Greenhouse M. A., Hayward T. L., Houck J. R., Mason C. G. and Woodward C. E. (1992) The peculiar infrared temporal development of Nova Vulpeculae 1987 (QV Vulpeculae). *ApJ*, **400**, 671-680.

Gehrz R. D., Greenhouse M. A., Hayward T. L., Houck J. R., Mason C. G. and Woodward C. E. (1995) The infrared spectrum of the optically thin dust shell of V705 Cassiopeiae (Nova Cassiopeiae 1993). *ApJL*, **448**, L119-L122.

Gehrz R. D., Truran J. W., Williams R. E. and Starrfield S. (1998) Nucleosynthesis in classical novae and its contribution to the interstellar medium. *PASP*, **110**, 3-26.

Gehrz R. D. (2008) Infrared studies of classical novae. In *Classical Novae* (eds. M. F. Bode and A. Evans), Cambridge University Press, Cambridge, Chapter 8, 167-193.

Gehrz R. D. Woodward C. E. Temim T. Lyke J. E. and Mason C. G. (2005) The development of a steady state, Asymptotic Giant Branch type, circumstellar wind around the "Born Again" Star FG Sagittae. *ApJ*, **623**, 1105-1114.

Gehrz R. D., Roellig T. L., Werner M. W., Fazio G. G., Houck J. R., Low F. J., Rieke G. H., Soifer B. T., Levine D. A. and Romana E. A. (2007) The NASA Spitzer Space Telescope. *Rev. Sci. Instrum.*, **78**, 011302-011339.

Gehrz R. D., Woodward C. E., Helton L. A., Polomski E. F., Hayward T. L., Houck J. R., Evans A., Krautter J., Shore S. N., Starrfield S., Truran J., Schwarz G. J. and Wagner R. M. (2008) The neon abundance in the ejecta of QU Vulpeculae from late-epoch infrared spectra. *ApJ*, **672**, 1167-1173.

Gehrz R. D., Evans, A., Helton L. A., Shenoy D. P., Banerjee D. P. K., Woodward C. E., Vacca W. D., Dykhoff D. A., Ashok N. M., Cass A. C., Carlon R. L., Corgan D. T., Eyres S. P. S., Joshi V., Keller L. D., Krautter J., Liimets T., Rushton M. and Starrfield S. (2015) The early infrared temporal development of Nova Delphini 2013 (V339 Del) observed with the Stratospheric Observatory for Infrared Astronomy (SOFIA) and from the ground. *ApJ*, **812**, 132(12pp).

Gehrz R. D., Evans A., Woodward C. E., Helton L. A., Banerjee D. P. K., Srivastava M. K., Ashok N. M., Joshi V., Eyres S. P. S., Krautter J., Kuin N. P. M., Page K. L., Osborne J. P., Schwarz G. J., Shenoy D. P., Shore S. N., Starrfield S. and Wagner R. M. (2018) The temporal development

of dust formation and destruction in Nova Sagittarii 2015#2 (V5668 Sgr): a panchromatic study. *ApJ*, **858**, 78(17pp).

Geisel S. L., Kleinmann D. E. and Low F. L. (1970) Infrared emission of novae. *ApJL*, **161**, L101-L104.

Gray C. M. and Compston W. (1974) Excess ^{26}Mg in the Allende meteorite *Nature*, **251**, 495-497.

Grishko V. I. and Duley W. W. (2002a) A 3.4 micron band in magnesium silicates: preparation of hydrocarbon-silicate condensates *ApJL*, **568**, L131–L134.

Grishko V. I. and Duley W. W. (2002b) Infrared absorption and emission spectra of hydrogenated amorphous carbon prepared in the presence of oxygen, nitrogen, ammonia, and carbon monoxide. *ApJ*, **568**, 448–453.

Gyngard F., Zinner E., Nittler L.R., Morgand A., Stadermann F. J. and Hynes K. M. (2010) Automated NanoSIMS measurements of spinel stardust from the Murray meteorite. *ApJ*, **717**, 107-10

Hadraoui K., Cottin H., Ivanovski S. L., Zapf P., Altwegg K., Benilan Y., Biver N., Della Corte V., Fray N., Lasue J., Merouane S., Rotundi A. and Zakharov, V. (2019) Distributed glycine in comet 67P/Churyumov-Gerasimenko. *A&A*, **630**, A32-A39.

Haenecour P., Floss C., José J., Amari S., Lodders K., Jadhav M., Wang A. and Gyngard F. (2016) Coordinated analysis of two graphite grains from the CO3.0 LAP 031117 meteorite: first identification of a CO nova graphite and a presolar iron sulfide subgrain. *ApJ*, **825**, 88-96.

Haenecour P., Howe J. Y., Zega T. J., Amari S., Lodders K., José J., Kaji K., Sunaoshi T. and Muto A. (2019) Laboratory evidence for co-condensed oxygen- and carbon-rich meteoritic stardust from nova outbursts. *Nature Astronomy*, **3**, 626-630.

Helton L. A., Woodward C. E., Walter F. M., Vanlandingham K., Schwarz G. J., Evans A., Ness J.-U., Geballe T. R., Gehrz R. D., Greenhouse M., Krautter J., Liller W., Lynch D. K., Rudy R. J., Shore S. N., Starrfield S. and Truran J. (2010) The dusty nova V1065 Centauri (Nova Cen 2007): a

spectroscopic analysis of abundances and dust properties. *AJ*, **140**, 1347-1369.

Helton L. A., Evans A., Woodward C. E. and Gehrz R. D. (2011) Atypical dust species in the ejecta of classical novae. In PAHs and the Universe, eds C. Joblin, A. G. G. M. Tielens, EAS Publications Series, **46**, 407-412.

Helton L. A., Gehrz R. D., Woodward C. E., Wagner R. M., Vacca W. D., Evans A., Krautter J., Schwarz G. J., Shenoy D. S. and Starrfield S. (2012) Elemental abundances in the ejecta of old classical novae from late-epoch Spitzer spectra. *ApJ*, **755**, 37(21pp).

Helton L. A., Evans A., Woodward C. E., Gehrz R. D. and Vacca W. (2014) The dusty nova: an examination of dust production and processing in the ejecta of classical novae. In Stella Novae: Past and Future Decades, eds P. A. Woudt and V. A. R. M. Ribeiro, ASP Conference Series, **490**, 261-266.

Herwig F. (2001) The evolutionary timescale of Sakurai's Object: a test of convection theory? *ApJL*, **554**, L71-L74.

Herwig F., Pignatari M., Woodward P. R., Porter D. H., Rockefeller G., Fryer C. L., Bennett M. and Hirschi R. (2011) Convective-reactive proton-^{12}C combustion in Sakurai's Object (V4334 Sagittarii) and implications for the evolution and yields from the first generations of stars. *ApJ*, **727**, 89(15pp).

Hinkle K. H., Lebzelter T., Joyce R. R., Ridgway S., Close L., Hron J. and Andre, K. (2008) Imaging ejecta from the final flash star V605 Aquilae. *A&A*, **479**, 817-826.

Höfner S. and Olofsson H. (2018) Mass loss of stars on the asymptotic giant branch. Mechanisms, models and measurements. *A&A Review*, **26**, 1-92.

Hora J. L., Latter W. B., Smith H. A. and Marengo M. (2006) Infrared observations of the Helix Planetary Nebula. *ApJ*, **652**, 426-441.

Houck J. R., Roellig T. L., van Cleve J., Forrest W. J., Herter T., Lawrence C. R., Matthews K., Reitsema H. J., Soifer B. T., Watson D. M., Weedman D.. Huisjen M., Troeltzsch J., Barry D. J., Bernard-Salas J., Blacken C. E., Brandl B. R., Charmandaris V., Devost D., Gull G. E., Hall P., Henderson C. P., Higdon S. J. U., Pirger B. E., Schoenwald J., Sloan G. C., Uchida

K. I., Appleton P. N., Armus L., Burgdorf M. J., Fajardo-Acosta S. B., Grillmair C. J., Ingalls J. G., Morris P. W. and Teplitz H. I. (2004) The Infrared Spectrograph (IRS) on the Spitzer Space Telescope. *ApJS*, **154**, 18-24.

Hyland, A. R. and McGregor P. J. (1989) PAH emission from nova Cen 1986. In IAU Symposium 135 Interstellar Dust, contributed papers, 101-106.

Iben I. (1982) Low mass asymptotic giant branch evolution. I. *ApJ*, **260**, 821-837.

Iliadis C., Downen L. N., José J., Nittler L. R. and Starrfield S. (2018) On presolar stardust grains from CO classical novae. *ApJ*, **855**, 76(14pp)

Ivezic Ž., Nenkova M. and Elitzur M. (1999) DUSTY: Radiation transport in a dusty environment. Astrophysics Source Code Library, record ascl:9911.001

Jadhav M., Pignatari M., Herwig F., Zinner E., Gallino R. and Huss G. R. (2013) Relics of ancient post-AGB stars in a primitive meteorite. *ApJL*, **777**, L27(7pp).

Jeffery C. S. and Schönberner D. (2006) Stellar archaeology: the evolving spectrum of FG Sagittae. *A&A*, **459**, 885-899.

Jiménez-Serra I., Testi L., Caselli P. and Viti S. (2014) Detectability of glycine in solar-type system precursors. *ApJL*, **787**, L33(5pp).

José J., Hernanz M. Amari S., Lodders K. and Zinner E. (2004) The Imprint of Nova Nucleosynthesis in Presolar Grains. *ApJ*, **612**, 414-428.

José J., Halabi G. M. and El Eid M. F. (2016) Synthesis of C-rich dust in CO nova outbursts. *A&A*, **593**, A54-A58.

José J., Shore S. N. and Casanova J. (2020) 123–321 models of classical novae. *A&A*, **634**, A5-A12.

Kawakita H., Jujii M., Nagashima M., Kajikawa T., Kuba N. and Arai A. (2015) Formation of C_2 and CN in nova V2676 Oph around its visual brightness maximum. *PASJ*, **62**, 17-24.

Kelley M. S. P., Harker D. E., Woodward C. E. and Wooden D. H. (2012) *Spitzer Space Telescope* Spectroscopy of Comets. urn:nasa:pds:spitzer:spitzer-spec-comet::1.0, NASA Planetary Data System.

Kessler M. F., Steinz J. A., Anderegg M. E., Clavel J., Drechsel G., Estaria P., Faelker J., Riedinger J. R., Robson A., Taylor B. G. and Ximenez de Ferran, S. (1996) The Infrared Space Observatory (ISO) mission *A&A*, **315**, L27-L31

Kraft R. P. (1964) Binary stars among cataclysmic variables. III. Ten old novae. *ApJ*, **139**, 457-475

Kwok S. (2016) Complex organics in space from Solar System to distant galaxies. *Astron. Astrophys. Rev.*, **24**, 8-34

Lawlor T. M. and MacDonald F. (2003) Sakurai's Object, V605 Aquilae, and FG Sagittae: an evolutionary sequence revealed. *ApJ*, **583**, 913-922

Leitner J. and Hoppe P. (2019) A new population of dust from stellar explosions among meteoritic stardust. *Nature Astronomy*, **3**, 725-729

Lisse C. M., VanCleve J., Adams A. C., A'Hearn M. F., Fernández Y. R., Farnham T. L., Armus L., Grillmair C. J., Ingalls J., Belton M. J. S., Groussin O., McFadden L. A., Meech K. J., Schultz P. H., Clark B. C., Feaga L. M. and Sunshine J. M. (2006) Spitzer spectral observations of the Deep Impact ejecta. *Science*, **313**, 635-640

Lisse C. M., Kraemer K. E., Nuth J. A., Li A. and Joswiak D. (2007) Comparison of the composition of the Tempel 1 ejecta to the dust in Comet C/Hale?Bopp 1995 O1 and YSO HD 100546 *Icarus*, **187**, 69-86

Lisse C. M. (2008) Rebuttal to "Comment on the paper "Comparison of the composition of the Tempel 1 ejecta to the dust in Comet C/Hale?Bopp 1995 O1 and YSO HD 100546" " *Icarus*, **195**, 941-944

Liu N, Nittler L. R., Alexander C. M. O'D., Wang J., Pignatari M., José J. and Nguyen A. (2016) Stellar origins of extremely ^{13}C- and ^{15}N-enriched presolar SiC grains: novae or supernovae? *ApJ*, **820**, 140(14pp).

Lodders K. (2003) Solar System abundances and condensation temperatures of the elements. *ApJ*, **591**, 1220-1247.

Loreta E. (1935) Nota sulle stelle variabili R Coronidi. *Astronomische Nachrichten*, **254**, 151.

Lund M. B., Siverd R. J., Pepper J. A. and Stassun K. G. (2016) Metrics for optimization of large synoptic survey telescope observations of stellar variables and transients. *PASP*, **128**, 025002-025011.

Lynch D. K., Woodward C. E., Gehrz R., Helton L. A., Rudy R. J., Russell R. W., Pearson R., Venturini C. C., Mazuk S., Rayner J., Ness J.-U., Starrfield S., Wagner R. M., Osborne J. P., Page K., Puetter R. C., Perry R. B., Schwarz G., Vanlandingham K., Black J., Bode M., Evans A., Geballe T., Greenhouse M., Hauschildt P., Krautter J., Liller W., Lyke J., Truran J., Kerr, T., Eyres S. P. S. and Shore S. N. (2008) Nova V2362 Cygni (Nova Cygni 2006): Spitzer, Swift, and ground-based spectral evolution. *AJ*, **136**, 1815-1827.

Mason C. G., Gehrz R. D., Woodward C. E., Smilowitz J. B., Greenhouse M. A., Hayward T. L. and Houck, J. R. (1996) Infrared observations of dust formation and coronal emission in Nova Aquilae 1995. *ApJ*, **470**, 577-582.

Mason C. G., Gehrz R. D., Woodward C. E., Smilowitz J. B., Hayward T. L. and Houck, J. R. (1998) The infrared development of V705 Cassiopeiae. *ApJ*, **494**, 783-791.

McLaughlin D. B. (1935) Remarks on Nova Herculis. *Publ. AAS*, **8**, 145-146.

McGuire B. A., Loomis R. A., Burkhardt A. M., Lee K. L. K., Shingledecker C. N., Charnley S. B., Cooke I. R., Cordiner M. A., Herbst E., Kalenskii S., Siebert M. A., Willis E. R., Xue C., Remijan A. J. and McCarthy M. C. (2021) Detection of two interstellar Polycyclic Aromatic Hydrocarbons via spectral matched filtering. *Science*, **371**, 1265-1269.

Messenger S. (2002) Opportunities for the stratospheric collection of dust from several short period comets. *Meteorit. Planet. Sci.*, bf 37, 1491-1505.

Mitchell R. M. and Evans A. (1984) Grain growth and destruction in novae. *MNRAS*, **209**, 945-954.

Molster F. J., Waters L. B. F. M., Tielens A. G. G. M. and Barlow M. J. (2002) Crystalline silicate dust around evolved stars. I. The sample stars. *A&A*, **382**, 184-221.

Nagashima M., Arai A., Kajikawa T., Kawakita H., Kitao E., Arasaki T., Taguchi G. and Ikeda Y. (2014) The transient molecular envelope in the outflow of the Nova V2676 Oph during its early phase. *ApJL*, **780**, L26(4pp).

Ney E. P. and Hatfield B. F. (1978). The isothermal dust condensation of Nova Vulpeculae 1976. *ApJL*, **219**, L111-L115.

Nittler L. R. and Hoppe, P. (2004a) New presolar silicon carbide grains with nova isotope signatures. 35th Lunar and Planetary Science Conference, abstract no. 1598.

Nittler L. R. and Hoppe, P. (2004b) High initial ^{26}Al/^{27}Al ratios in presolar SiC grains from novae. *Meteor. & Plan. Sci.*, **39**, abstract no. 5060

Nuth J. A. and Hecht J. H. (1990) Signatures of aging silicate dust. *Ap&SpSci.*, **163**, 79-94.

O'Keefe J. A. (1939) Remarks on Loreta's hypothesis concerning R Coronae Borealis. *ApJ*, **90**, 294-300.

Ootsubo T., Kawakita H., Shinnaka Y., Watanabe J. and Honda M. (2020) Unidentified infrared emission features in mid-infrared spectrum of comet 21P/Giacobini-Zinner. *Icarus*, **338**, 113450-113456.

Pavlenko Ya. V., Geballe T. R., Evans A., Smalley B., Eyres S. P. S., Tyne V. H. and Yakovina L. A., (2004) CO bands in V4334 Sgr (Sakurai's Object): The ^{12}C/^{13}C ratio. *A&A*, **417**, L39-L43.

Pavlenko Ya. V., Evans A., Banerjee D. P. K., Geballe T. R., Munari U., Gehrz R. D., Woodward C. E. and Starrfield S. (2020) Isotopic ratios in the red giant component of the recurrent nova T Coronae Borealis. *MNRAS*, **498**, 4853-4863.

Peeters E., Hony S., Van Kerckhoven C., Tielens A. G. G. M., Allamandola L. J., Hudgins D. M. and Bauschlicher C. W. (2002) The rich 6 to 9 μm spectrum of interstellar PAHs. *A&A*, **390**, 1089-1113.

Pepin R. O., Palma R. L., Gehrz R. D. and Starrfield S. (2011) Presolar grains from novae: evidence from neon and helium isotopes in comet dust collections. *ApJ*, **742**, 86-100.

Phillips J. P. (1984) The dynamics, evolution and formation rate of planetary nebulae *A&A*, **197**, 92-100.

Pontefract M. and Rawlings J. M. C. (2004) The early chemical evolution of nova outflows. *MNRAS*, **347**, 1294-1303.

Rauscher D. M., Heger A., Hoffman R. D. and Woosley S. E. (2002) Nucleosynthesis in massive stars with improved nuclear and stellar physics. *ApJ*, **576**, 323-348.

Rawlings J. M. C. (1988) Chemistry in the ejecta of novae. *MNRAS*, **232**, 507-524.

Rawlings J. M. C. and Williams D. A. (1989) Chemical routes to dust formation in the ejecta of novae. *MNRAS*, **240**, 729-740.

Saikia D. J. and Anupama G. C. (2012) Novae: from Radio to Gamma Rays, special edition of the Bulletin of the Astonomical Society of India, **40**, 161-456.

Sakon I., Sako S., Onaka T., Nozawa T., Kimura Y., Fujiyoshi Takuya., Shimonishi T., Usui F., Takahashi H., Ohsawa R., Arai A., Uemura M., Nagayama T., Koo B.-C. and Kozasa T. (2016) Concurrent formation of carbon and silicate dust in Nova V1280 Sco. *ApJ*, **817**, 145(23pp).

Schaefer B. E. (2018) The distances to novae as seen by *Gaia MNRAS*, **481**, 3033-3051

Shafter A. W. (2017) The Galactic nova rate revisited *ApJ*, **834**, 196(11pp).

Shore S. N., Starrfield S., Gonzalez-Riestra R., Hauschildt P. H., and Sonneborn G. (1994) Dust formation in Nova Cassiopeiae 1993 seen by ultraviolet absorption *Nature*, **369**, 539-541.

Sloan G. C., Jura M., Duley W. W., Kraemer K. E. Bernard-Sala, J., Forrest W. J., Sargent B., Li A., Barry D. J., Bohac C. J., Watson D. M. and Houck J. R. (2007) The Unusual Hydrocarbon Emission from the Early Carbon

Star HD 100764: The Connection between Aromatics and Aliphatics. *ApJ*, **664**, 1144-1153.

Smith C. H., Aitken D. K. and Roche P. F. (1994) The mid-infrared spectral development of Nova Cen 1986. *MNRAS*, **267**, 225-230.

Snijders M. A. J., Batt T. J., Roche P. F., Seaton M. J., Morton D. C., Spoelstra T. A. T. and Blades J. C. (1987) Nova Aquilae 1982. *MNRAS*, **228**, 329-376.

Starrfield S., Gehrz R. D. and Truran J. W. (1997) Dust formation and nucleosynthesis in the nova outburst. In Astrophysical implications of the laboratory study of presolar materials (eds. T. J. Bernatowicz, E. Zinner) *AIPC*, **403**, 203-234.

Starrfield S., Iliadis C., Hix W. R., Timmes F. X. and Sparks W. M. (2009) The effects of the *pep* nuclear reaction and other improvements in the nuclear reaction rate library on simulations of the classical nova outburst. *ApJ*, **692**, 1532-1542.

Starrfield S., Bose M., Iliadis C., Hix W. R., Woodward C. E. and Wagner R. M. (2020) Carbon-Oxygen classical novae are Galactic ^{7}Li producers as well as potential Supernova Ia progenitors. *ApJ*, **895**, 70(24pp).

Strope R. J., Schaefer B. E. and Henden A. A. (2010) Catalog of 93 nova light curves: classification and properties. *AJ*, **140**, 34-62.

Suzuki T., Ohishi M., Hirota T., Saito M., Majumdar L. and Wakelam V. (2016) Survey observations of a possible glycine precursor, methanimine (CH_2NH) *ApJ*, **825**, 79(14pp).

Tielens A. G. G. M. (2008) Interstellar Polycyclic Aromatic Hydrocarbon Molecules. *ARA&A*, **46**, 289-337.

Tyne V. H., Evans A., Geballe T. R., Eyres S. P. S., Smalley B. and Dürbeck H. W. (2002) Sakurai's Object (V4334 Sgr): evolution of the dust shell from 1999 to 2001. *MNRAS*, **334**, 875-882.

Vaytet N. M. H., O'Brien T., J.and Rushton A. P. (2007) Evidence for ablated flows in the shell of the nova DQ Herculis. *MNRAS*, **380**, 175-180.

Wada S., Onaka T., Yamamura I., Murata Y. and Tokunaga A. T. (2003) ^{13}C isotope effects on infrared bands of quenched carbonaceous composite (QCC). *A&A*, **407**, 551-562.

Werner K. and Herwig F. (2006) The Elemental Abundances in Bare Planetary Nebula Central Stars and the Shell Burning in AGB Stars. *Publications of the Astonomical Society of the Pacific*, **118**, 183-204.

Werner M. W. Roellig T. L., Low F. J., Rieke G. H., Rieke M., Hoffmann W. F., Young E., Houck J. R., Brandl B., Fazio G. G., Hora J. L., Gehrz R. D., Helou G., Soifer B. T., Stauffer J., Keene J., Eisenhardt P., Gallagher D., Gautier T. N., Irace W., Lawrence C. R. Simmons L., Van Cleve J. E., Jura M., Wright E. L. and Cruikshank D. P. (2004) The Spitzer Space Telescope Mission. *ApJS*, **154**, 1-9.

Williams D. M., Mason C. G., Gehrz R. D., Jones T. J., Woodward C. E., Harker D. E., Hanner M. S., Wooden D. H., Witteborn F. C. and Butner H. M. (1997) Measurement of Submicron Grains in the Coma of Comet Hale-Bopp C/1995 01 during 1997 February 15–20 UT. *ApJL*, **489**, L91-L94

Woodward C. E., Gehrz R. D., Jones T. J. and Lawrence G. F. (1992) The peculiar, fast Nova Herculis 1991. *ApJL*, **384**, L41-L45.

Worters, H. L., Rushton M. T., Eyres S. P. S., Geballe T. R. and Evans A. (2009) Sakurai's Object: characterizing the near-infrared CO ejecta between 2003 and 2007. *MNRAS*, **393**, 108-112.

Woudt P. and Riberio V. A. R. M. (2014) Stella Novae: Past and Future Decades, Astronomical Society of the Pacific Conference Series, volume **490**, San Francisco.